Fall 2019

Innovative Approaches Using Multispectral Imagery to Detect Nearshore Bars and Elucidate Beach-Dune System Dynamics

Mayra A. Román-Rivera

INNOVATIVE APPROACHES USING MULTISPECTRAL IMAGERY TO DETECT NEARSHORE BARS AND ELUCIDATE BEACH-DUNE SYSTEM DYNAMICS

by

Mayra A. Román-Rivera

Bachelor of Arts
University of Puerto Rico, Rio Piedras Campus, 2012

Master of Arts
East Carolina University, 2014

Submitted in Partial Fulfillment of the Requirements

For the Degree of Doctor of Philosophy in

Geography

College of Arts and Sciences

University of South Carolina

2019

Accepted by:

Jean T. Ellis, Major Professor

Thomas R. Allen, Committee Member

April L. Hiscox, Committee Member

Cuizhen Wang, Committee Member

Cheryl L. Addy, Vice Provost and Dean of the Graduate School

DEDICATION

I would like to dedicate this work to my family who inspired and encouraged me to follow my dreams. From summer walks searching for fossils in the mountains, to blissful strolls in the beach collecting beach glass you instilled in me a sense of curiosity and inquiry that has guided me to this day. To my aunts, Odalys and Lucy Rivera, thank you for gifting me books that introduced me to maps, critical thinking, and environmental issues at such a young age. I especially want to dedicate this dissertation to my parents Ismael Román and Betzaida Rivera and my siblings Glenda and Ismael Alberto Román, without your unwavering support I would be here. This work is yours as much as it is mine. I also want to dedicate this work to Nicholas Sokol. When the road got tough and I doubted everything, you were always by my side giving me all your support and love. I wouldn't have made it this far without you.

ACKNOWLEDGEMENTS

They said it take a village, that is certainly true when it comes to raising a scholar. First and foremost, I want to thank my advisor, Dr. Jean Ellis. These five years have been incredibly challenging for many reasons, but you have always been there for me every step of the way. I could not have chosen a better advisor and mentor to complete this journey with. I also want to thank my committee members Drs. Thomas Allen, April Hiscox, and Susan Wang your feedback and support throughout this process have been fundamental to my research.

I would also like to thank Drs. Gregory Carbone, Susan Cutter, Kirstin Dow, Amy Mills, and Caroline Nagel for their support. These professors were not part of my committee, yet they always were there for me to offer advice, write letters of recommendation, forward fellowship and scholarship opportunities, and to help me grow as a professional. To my WINDlab colleagues, past and present, thank you for keeping me sane and well fed.

Finally, I would like to thank the Department of Geography at the University of South Carolina, the American Association of Geographers, and the Southern Regional Education Board for providing funds that allowed me to complete my studies and my research.

ABSTRACT

Nearshore bars naturally protect the coast against erosion by dissipating wave energy. They are significant reservoirs of sand, and thus, they may impact the response of beaches to different wave conditions. Nearshore bar position and morphologic variability also influences long- and short-term beach and dune stability. This study reveals how nearshore bars influence beach-dune dynamics using very high-resolution (VHR) imagery. A new low-cost identification approach for bar identification was applied by integrating VHR imagery. Future nearshore bar research will benefit from integrating the larger spatial scale provided by satellite sensors. A rule-based OBIA approach was successful in identifying and characterizing nearshore bars. This study also looked at the interactions of nearshore dynamics and the beach-dune system by investigating the coastal system holistically instead of each feature (dunes, beach, and bars) as separate entities. Knowing how the dunes, the beach and the bars dynamics are related and how each component affects the response of the other during high-energy wave event conditions will also significantly improve the way that we manage, protect, and develop our coastlines. Results showed that the morphology of the nearshore bars have a direct impact on how the dune-beach system respond to high-energy events.

TABLE OF CONTENTS

LIST OF TABLES

LIST OF FIGURES

CHAPTER 1

INTRODUCTION

This dissertation aims to study how nearshore bars influence beach-dune dynamics by using multispectral imagery. The research focuses on nearshore bars because understanding the system's interaction with the beach-dune system is important to develop conservation and management plans based on their unique dynamics and patterns. Although nearshore bars have been studied previously, questions remain regarding their influence over the beach-dune system. Due to their location they are more challenging to study and therefore will benefit from improved techniques to investigate them. This remote sensing-based method for nearshore bar identification will increase the spatial and temporal capability to study nearshore bar systems at a decreased cost compared to *in situ* projects. This research also explores how nearshore bars respond to high-energy wave events, such as tropical cyclones and winter storms, and their efficacy in protecting the dunes and the beach. The dissertation specifically looks at how distinct bar morphologies protect the subaerial beach differently. The ultimate goal is to streamline the process of assessing and monitoring coastal landscapes.

Chapters 2, 3 and 4 will be published as three separate manuscripts. Chapter 2 includes a review of all the methods previously used to monitor and study coastal systems. Chapter 3 introduces and discusses a rule-based OBIA approach to identify nearshore bars and verifies the data obtained using Argus imagery. Lastly, Chapter 4 looks into the

responses of nearshore bars to high-energy wave events and their efficacy in protecting the dune and beach.

1 Hypotheses and objectives

This dissertation research is guided by two hypotheses (Table 1.1). The first hypothesis and the associated objectives relates to applying and testing a bar identification approach based on VHR multispectral imagery. VHR multispectral images have high spatial resolution, and therefore an accurate identification of nearshore bars is possible. This method incorporates an existing and widely accepted bar classification scheme (Lippmann and Holman, 1990). The second hypothesis and associated objectives employ the rule-based OBIA approach from the previous hypothesis. This portion of the study focuses around high-energy wave events to holistically understand the interactions between nearshore dynamics and the beach-dune system.

Table 1.1 Summary of research hypotheses and objectives

Hypotheses	Objectives
A rule-based OBIA approach can be applied to multispectral imagery to identify nearshore bars.	• Acquire nearshore bar characteristics for three locations. • Compare the accuracy of multispectral images of the rule-based OBIA nearshore bar identification. approach using the Argus video monitoring system. • Calculate percentage of error for bar identification.
Bar morphology influences beach-dune characteristics and this relationship varies geographically.	• Measure bar morphology and beach-dune characteristics using multispectral imagery. • Establish if coastal system components vary geographically. • Quantify bar morphology and characteristics, and coastal system responses during high-energy wave event conditions.

2 Research Broader Impacts

The field of coastal geomorphology studies the dynamics and processes that occur in coastal regions. Understanding the spatiotemporal scale at which nearshore bar systems evolve and how those patterns are related to beach-dune response are important to create effective coastal management plans. Knowing how the dunes, the beach, and the bars dynamics are related and how each component affects the response of the other during high-energy wave event conditions will significantly improve the way that we manage, protect, and develop our coastlines. This novel approach for nearshore bar identification will increase the spatial and temporal capability to study nearshore bar systems at a decreased cost compared to *in situ* projects. Understanding the relationship between the dune, beach, and nearshore bars and how the system responds to high-energy events can provide managers with means to identify areas of erosion and better protect those areas and surrounding infrastructures. Integrating traditional remote sensing technology (multispectral imagery) with newer and innovative techniques for coastal management and studies will increase accessibility to researchers and coastal management.

CHAPTER 2

A SYNTHETIC REVIEW OF REMOTE SENSING APPLICATIONS TO DETECT NEARSHORE BARS[1]

---

[1]Román-Rivera, M.A. & Ellis, J.T. 2019. *Marine Geology.* 408: 144-153. Reprinted here with permission of publisher.

1 Introduction

The nearshore is defined as a transition zone between the land and the continental shelf and is significantly influenced by waves during normal and extreme conditions (i.e., tropical cyclones and winter storms). It represents an important and highly dynamic region of the coastal system. The nearshore is vital to the economy, security, commerce, and recreation of all coastal nations (Barbier et al., 2008; Borja, 2005; Dugan et al., 2011; Elko and Holman, 2014; Holman et al., 2003). This region is constantly evolving, is often densely populated, and is threatened by long-term erosion caused by sea level rise, the impact of storms, and anthropogenic influences (Elko and Holman, 2014).

Nearshore processes, such as sediment and water movement generated by waves and currents, play an important role in determining the morphodynamic state of the beach. These processes shape the overall geometry of the foreshore, beach slope, grain distribution, and beach width (Houser and Ellis, 2013; Rutten et al., 2018; Sherman and Bauer, 1993). Nearshore characteristics (i.e., presence or absence of bars, bar count, and slope) regulate sediment delivery to the subaerial beach (Bauer, 1991; Pye, 1982; Sherman and Bauer, 1993). In turn, the morphodynamic beach state has important implications for beach-dune sediment exchange (Houser, 2009; Sherman and Bauer, 1993). Sediment characteristics of the nearshore, such as grain size, volume, and distribution are crucial to aeolian processes and resulting landforms on the subaerial beach (Houser and Greenwood, 2007; Houser and Ellis, 2013; Rutten et al., 2018; Sherman and Bauer, 1993). Bar morphodynamics can provide a better understanding of the subaerial beach-dune systems dynamics.

In this article, we summarize the use of remote sensing imagery to study bar morphodynamics (Figure 2.1). Others have compiled comprehensive reviews of bar

dynamics (c.f. Cohn et al., 2014; Davidson-Arnott, 2013; Falqués et al., 2008). The following sections outline the parameters required to effectively employ still and video photography (Argus and surfcams) and satellite imagery for bar identification. Lastly, we discuss the benefits and limitations associated with each monitoring method and suggest future research directions.

2 Nearshore bar research

Our efforts to understand bar morphodynamics can be traced back to the early 1900s (Evans, 1940; King and Williams, 1948). It was not until the mid-1970s that sensors, aerial photography, and other computer-based technologies were employed to study this region with higher precision (Carter and Balsillie, 1983; Carter and Kitcher, 1979; Greenwood and Davidson-Arnott, 1979; Short and Hesp, 1982). Since then, we have been able to provide a more thorough understanding of these dynamic morphologies. Advances in technology, in combination with instrument intensive field experiments (i.e., Aagaard et al., 1998; Holman and Sallenger, 1993; Huntley and Bowen, 1973; Sherman and Greenwood, 1984), led to the development of theoretical and numerical models (e.g., Aagaard and Masselink, 1999; Greenwood and Davidson-Arnott, 1979; Wijinberg and Kroon, 2002) of water motion and sediment transport that substantially contributed to the understanding of the mechanisms that may lead to bar formation.

Advances in *in situ* methods have made the task of repeatedly measuring bars easier, but these methods are still time-consuming, expensive, and spatially limited (Holman and Haller, 2013; Holman and Stanley, 2007). In addition, field based experiments are often temporally limited because of harsh conditions in the surf zone.

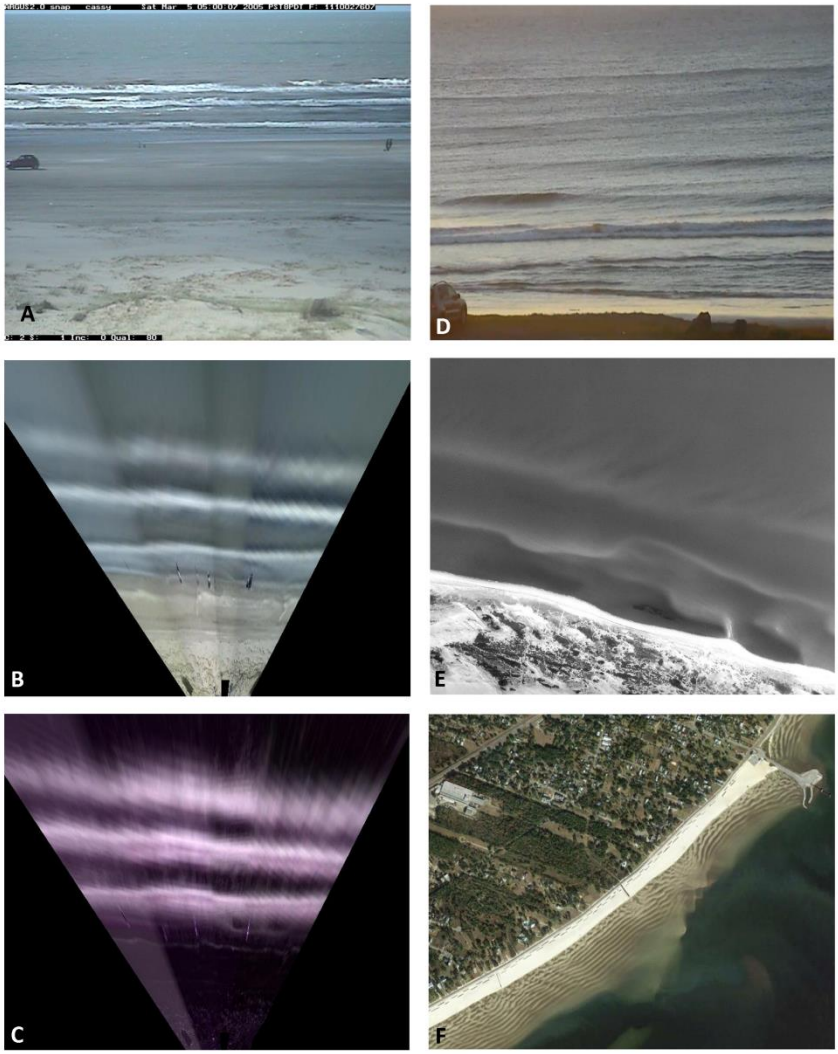

Figure 2.1 Examples of near-Earth and satellite image products. A, B, and C are Argus products from Cassino Beach, Brazil A) Snapshot from their camera 2 that shows waves breaking over the bars; B) Timex image; C) 10-minute variance image; D) Snapshot of a surfcam located at Coffs Harbour, Australia; E) 1990 aerial image of the nearshore bars near Province Lands, Cape Cod, MA; F) Landsat-8 natural color image showing the bar system in Bay St. Louis, MS (obtained on 11/26/2014).

Breaking waves and wave-driven currents in the surf zone are potentially dangerous for divers and frequently result in instrument failure (Holman and Haller, 2013; Lippmann and Holman, 1989). Sandy bottoms may undergo substantial erosion or accretion over a short period of time, which could rapidly scour or bury bottom-mounted sensors and

adversely affect data collection. Lastly, water-level changes related to tidal fluctuations at the study site can also affect instrumentation by changing the fixed sensor's domain range (Holman and Haller, 2013). All these limitations can be overcome by employing remote sensing technologies.

Remote sensing techniques permit the collection of repetitive bar surveys at longer-time scales (months to years), compared to *in situ* experiments. These techniques provide a cost-effective option that allow for the systematic and worldwide study of bar systems under environmentally harsh conditions. They also have provided a wealth of data on bar formation, evolution, and characteristics (c.f., Aarninkhof et al., 2000; Aleman et al., 2017; Alexander and Holman, 2004; Konicki and Holman, 2000; Lippmann and Holman, 1989, 1990; Plant et al., 1997; Ribas et al., 2010; Ruessink et al., 2002; Sonu, 1972). Coastal geomorphologists have ascertained substantial conclusions from qualitative and quantitative remotely-based observations suggesting the processes controlling the formation and evolution of bars (Alexander and Holman, 2004; Houser and Greenwood, 2007; Konicki and Holman, 2000; Lippmann and Holman, 1990; Ruessink et al., 2002). Imagery obtained from remote sensing instruments is particularly appealing because remote instrumentation alleviates many of the challenges related to *in situ* instrumentation (Holland et al., 1997).

3 Remote sensing methods to study bar morphodynamics

Multiple types of remote sensing technologies have been used to study bar morphodynamics and the surrounding hydrodynamics (Holman and Haller, 2013; Holman and Stanley, 2007; Ribas et al., 2017). Active and passive remotely sensed instruments, such as cameras, radars,

and light detecting and ranging systems (Lidar), have been employed to conduct these investigations. Sensors can be mounted on different platforms depending on the application; they can be fixed, flying, floating or, in the case of satellite imagery, orbiting the Earth. Bar monitoring programs must have ample temporal frequency and duration to differentiate between the short- (days to weeks) and long-term (months to years) evolution of bar systems to capture changes in the system that occur in response to a high energy event versus gradual changes in the system (Aleman et al., 2017; Lippmann and Holman, 1990). Bar morphology studies employing remote sensing should satisfy the following criteria: a) the shape of the bar must be easily identifiable; b) the position of the crest must be measured accurately over a range of longshore distances; and c) the sampling must be possible across a range of hydrodynamic conditions (Lippmann and Holman, 1990). The remote sensing techniques discussed in the following sections, aerial photography, video monitoring systems, and satellite imagery, all conform to the criteria described above.

3.1 Aerial photography

Near-Earth imagery can be obtained with minimal interference to the environment and generally requires less logistical efforts compared to field experiments (van Dongeren et al., 2008). These monitoring techniques operate under the principle of optimizing the optical signatures of nearshore surfaces. For example, the location of concentrated wave breaking may indicate the position of submerged bars (Holman et al., 2003; Holman and Stanley, 2007). Near-Earth imagery comprises still camera imagery and videography, discussed below.

Aerial photography (Figure 2.1E) has been used to track bar morphodynamics since the early 1900s. This technique replaced the plane table survey method for shoreline

mapping, since aerial photography can cover extensive areas with greater detail while maintaining the horizontal control of the plane table survey method (Liu et al., 2007). Since the early 1920s, the National Oceanic Service (NOS), office within the United States National Oceanic and Atmospheric Administration (NOAA) has been tasked with investigating the feasibility of using aerial photography to compile coastal topography (Graham et al., 2003; Liu et al., 2007). Early work proved that aerial photographs were useful for obtaining topographical information (Harris and Umbach, 1972; Lundahl, 1948; Wiegel, 1947). Aerial photography proved to be a more accurate and time-effective method to collect shoreline data. Researchers and agencies were able to bring shoreline compilations from the field to the office (Graham et al., 2003; Liu et al., 2007). Some U.S. coastal regions have an extensive record of aerial photography, which can serve to study long-term variability of nearshore bars (Moore, 2000; Sheppard et al., 1995). In some regions, black and white aerial photographs date back to the 1920s, but research-quality stereo photographs (two or more offset photographs that allow the estimation of 3-D coordinates of points by creating or enhancing the perception of depth in an image) were not available until the early 1940s (Harris and Umbach, 1972; Moore, 2000). High resolution (1.0 – 5.0m) aerial photography and images are currently available at a low cost through federal and state government agencies, at map libraries, and for a fee from commercial entities.

Still camera systems are used because of their high speed and spatial resolution. Images typically results in higher quality compared to standard video systems (Coco et al., 2005). For example, a still camera system installed at Lowestoft, UK, has the capability to stream 6-7 frames per second and capture and save images to a disk at a rate of two frames per second (Coco et al., 2005). These high-resolution images improve the ability to discern

bar features. Still cameras can be programmed to acquire oblique snapshots during daylight hours at pre-determined time intervals. The bar locations are interpreted from the discontinuous foam associated with breaking waves in the individual snapshots (Konicki and Holman, 2000; Plant and Holman, 1997). Merging or stacking multiple images provides average natural modulations of the nearshore wave field, which has been shown to be an accurate proxy for the underlying, submerged bar topography (Aarninkhof et al., 2000; Lippmann and Holman, 1990; Plant and Holman, 1997). These merged images can also provide bar count, width and length, as well as shoreline orientation and width (Aarninkhof et al., 2000; Konicki and Holman, 2000; Lippmann and Holman, 1989).

One product of the Argus cameras, which is discussed in detail in the next section, is the single (still) snapshot (Figure 2.1A). The Argus snapshots are remotely triggered, usually at 2 Hz, to capture images at the top of every daylight hour. The network of Argus beach cameras are temporally synchronous and therefore able to detect waves (Armaroli and Ciavola, 2011; Holman and Stanley, 2007). The temporal resolution of the Argus system reduces errors associated with non-stationarity since the sampling rate is faster than the observed rate of bar movement (Lippmann and Holman, 1989). Snapshots provide effective and routine qualitative synoptic assessments of bar morphodynamics.

To use near-Earth imagery for qualitative analysis, the products must be referenced in space and corrected for lens distortion. This process, called geo-rectification, requires identification of ground control points (GCP) in the image and in the real world (Archetti and Zanuttigh, 2010; Holland et al., 1997). A minimum of eight to ten GCPs distributed throughout the study are needed to reduce image distortion (Holland et al., 1997; Moore, 2000; Thieler and Danforth, 1994). Increasing the number of GCPs will improve the

algorithms and reduce the geographic distortion of the image (Archetti and Zanuttigh, 2010; Holland et al., 1997; Moore et al., 2003). Identifying GCPs is often a challenge when studying bars because a substantial portion the image observes water. Fortunately, laboratory, based image corrections have been formulated and effectively implemented to provide setup and calibration of the camera system, including accounting for lens distortion and sampling imprecisions resulting from the digitization processes (Beyer, 1992; Holland et al., 1997; Penna, 1991; Plant et al., 2002).

The process of geo-rectification can be a source of uncertainty in the final dataset. Accounting for geo-rectification uncertainty has important implications when reporting the location of bars and their movement over time (Rodríguez-Martín and Rodríguez-Santalla, 2013). The rectified image error is estimated by comparing the distances between the 'real-world' GCPs and the image-derived GCPs (Archetti and Zanuttigh, 2010; Holland et al., 1997). The reported acceptable error ranges between 2.0 to 6.0 m (Moore, 2000; Roman-Rivera, 2014; Thieler and Danforth, 1994). After geo-rectification, additional processing of still camera imagery is often required to enhance the contrast between the bars and the surrounding deeper water (Moore et al., 2003).

Geometric corrections need to be frequently repeated when still cameras are used to compensate for the changes of the camera's field of view (FOV) (Archetti and Zanuttigh, 2010). Changes in the FOV can be caused by wind and temperature fluctuations, which cause minor movements to the system and, therefore, the focus of the lens (Archetti and Zanuttigh, 2010). Many cameras used to study bars are placed at a fixed location for long durations, which is advantageous because there is set viewing geometry (Holman and Haller, 2013; Holman and Stanley, 2007). In some instances, the fixed camera location may lack the

high vantage point and viewing angles needed for sampling at a particular spectral band and detecting different variables (i.e., breaking waves) (Holman and Haller, 2013; Lippmann and Holman, 1990). A potential limitation of these systems is that snapshots may omit time domain information, which could be needed for more sophisticated quantitative analysis (Holman et al., 2003). Another possible limitation is that not all still camera systems allow remote download of data. Many require connectivity to a computer via USB or Wi-Fi (Coco et al., 2005).

The digitization process, or the process of feature identification in the image, might also be a source of uncertainty, specifically the occurrence of sunglint and image contamination. Image contamination comes in multiple forms, which could prohibit bar identification or lead to erroneous bar characterizations. Optically complex waters (case 2) from phytoplankton, suspended sediment, and/or dissolved organic matter contaminate the image and prohibit bar identification. In clear water, color differences are used to identify shallower areas (i.e., the bars). However, changing sun angles and tidal stages create uncertainty surrounding the identification of the shade of sand that identifies the bar (Alexander and Holman, 2004; Plant and Holman, 1997). It is difficult to correct for sunglint, as its reflection saturates the sensor and obstructs the collection of any other spectral information. Fortunately, the effects of sunglint and image contamination can be reduced using image spectral enhancement, and filtering and texture techniques to ultimately improve bar identification (c.f., Shoshany and Degani, 1992).

While there is a definite spatial advantage to using still cameras, large uncertainties manifest when extrapolating findings from temporally limited observations (Lippmann and Holman, 1989; Moore, 2000; Thieler and Danforth, 1994). For example, Lippmann and

Holman (1989) explain that infrequent observations provide incomplete knowledge demonstrating the connection between instantaneous visual wave breaking patterns and the underlying local bathymetry. Aerial photography is collected at different time intervals depending on the location (could be consistently collected 1-2 times per year or only after a major event), making it challenging to conduct short-term research utilizing this technique. This forces the user of aerial photography to employ some level of subjectivity that leads to possible inconsistencies in the bar detection process (Shoshany and Degani, 1992).

3.2 Video monitoring

Coastal video systems were originally developed to improve scientific understanding of nearshore systems and their response to tidal and wave forcing (Davidson et al., 2007; Holman et al., 2003). Fixed video cameras mounted high above the beach affords a wide field of view that is ideal for monitoring bars, as well as the shoreline and rip currents (Davidson et al., 2007; Holman and Stanley, 2007). Video monitoring systems to study bar morphodynamics have been recognized by the scientific community, specifically through the use of Argus (c.f., Aarninkhof et al., 2003; Alexander and Holman, 2004; Guedes et al., 2011; Holman et al., 2015; Lippmann and Holman, 1989; Madsen and Plant, 2002; Plant and Holman, 1997; Wijnberg and Terwindt, 1995) and surfcams (c.f., Bracs et al., 2016; Brignone et al., 2012; Mole et al., 2013; Turner et al., 2006).

3.2.1 Argus system

The most frequently used video monitoring system to study bar morphodynamics is the Argus station developed by the Coastal Imaging Lab (CIL) at Oregon State University. Its purpose is "to provide a low-cost accessible system for sampling of the important

hydrodynamic forcing and bathymetric response variables in this range of nearshore environments" (Holman and Stanley, 2007, pp.485). Since its inception, the Argus coastal imaging system has expanded to an international effort, collecting imagery for almost three decades, and meeting a range of research and management needs (Bracs et al., 2016). Other video systems have since been developed and installed to monitor coastal systems, based on Argus utilities and software, such as Cam-Era (National Institute of Water and Atmospheric Research New Zealand) (c.f. Coco et al., 2005; van de Lageweg et al., 2013), Kosta System (Université de Pau et des Pays de l'Andor France) (c.f. Rihouey et al., 2009), CoastalCOMS (Coastal Conditions Observation and Monitoring Solutions, Australia) (c.f. Bracs et al., 2016; Murray et al., 2013; Splinter et al., 2011), and Horus (University of Cantabria Spain and National University of Colombia) (c.f. Garnier et al., 2012) (Nieto et al., 2010). Because of its overwhelming popularity in the literature, this review will focus on Argus.

An Argus station enables controlled acquisition and returns optical remote sensing data to land-based computers (Holman et al., 2003; Holman and Stanley, 2007). Argus stations comprise four to five video tower mounted cameras attached to a host computer that serves as the system control and a communication link between the cameras and the data archives. The cameras have a 1024x768 pixel resolution, a field of view spanning 180°, and an aim angle that is within 0.1 pixel or 0.004°. These parameters allow for a spatial coverage of 3-6 km of the nearshore (Aarninkhof et al., 2000; van Enckevort et al., 2004). Presently, there are approximately 50 operational sites in Australia, Brazil, England, Italy, Japan, the Netherlands, New Zealand, Spain and the United States. Argus cameras typically provide 30 images per second with each image containing approximately 768 kB of data (Holman and Stanley, 2007). Each camera typically collects 18 GB of data per day containing 12 runs

starting at the top of the hour and lasting 17 minutes. The Argus system has three sampling methods collected during 12 (assumed) daylight hours: a) single snapshots (see section 3.1); b) 10-minute time-exposures (or timex); and c) 10-minute variance images. Argus data has also been used to compare statistics of shoreline and bar variability (Alexander and Holman, 2004; van Enckevort et al., 2004).

One timex image (Figure 2.1B) is obtained per hour and each image represents the mathematical temporal-mean of all frames collected during the first 10 minutes of the hour using a 2Hz sampling rate (Holman and Stanley, 2007). The main use of timex images is to delineate areas of waves breaking in the surf zone obtained by averaging fluctuations due to incident wave modulations (Lippmann and Holman, 1989; Ribas et al., 2010; van Enckevort et al., 2004). Subsequently, these images can be used to approximate the location of bars, since the areas of concentrated breaking waves appear as white bands in the image. Calibration studies have demonstrated that the bar locations can be derived accurately from timex images (Holman and Stanley, 2007; Lippmann and Holman, 1989) by using site-specific parameters (wave height, tidal level, and slope) to define the relationship between wave breaking and bar crest position (Ribas et al., 2010). High-energy conditions may erroneously suggest substantial landward bar migration because of the presence of foam on the shoreward edge of the bar system (Lippmann and Holman, 1989). Image differencing or subtracting successive video frames and averaging the difference images can be used to remove persistent foam that is not associated with actively breaking waves, thus eliminating potential error (Guedes et al., 2011; Lippmann and Holman, 1990). The time interval between successive frames is 0.5 second, while the threshold noise level should be approximately 6% of the maximum range of intensity (Lippmann and Holman, 1990).

The third Argus product is the 10-minute variance image (Figure 2.1C). These are also generated from amalgamating the 2Hz single frame images collected during the first 10 minutes of each daylight hour. The 10-minute variance images result in brighter areas where there is a strong natural variation and therefore are often used to delineate the surf zone (Guedes et al., 2011; Holman et al., 2003; Holman and Stanley, 2007). Combining Argus timex and variance images provide optimal estimates of bar location, especially when hydrodynamic data are not available (Guedes et al., 2011). Analyzing the maximum wave energy dissipation and the maximum averaged pixel intensity may lead to stronger associations between the breaking wave patterns and the location of bars when the waves are small (Guedes et al., 2011; Lippmann and Holman, 1989). This method can therefore be used to study the morphology and dynamics of bar systems located in coastal areas characterized by lower wave heights and micro-tidal environments (Guedes et al., 2011; Ribas et al., 2010).

Since its inception, the Argus system has been extensively used to measure nearshore bathymetry and morphology. Lippmann and Holman (1989) were the first to model the relationship between the white bands in time-exposure images and the positions of underlying bar crests. Their model allowed for the visualization and quantification of nearshore morphology based on the patterns of incident wave breaking. Lippmann and Holman's model (1989) assumed that more waves break over the shallow water above the bar compared to the surrounding areas, creating a sharp contrast between breaking and non-breaking regions that may be photographed. Over the years, the Lippmann and Holman model has been improved by correcting discrepancies associated with changing tide elevations and wave heights (Kingston et al., 2000; van Enckevort and Ruessink, 2003).

Argus-specific analysis tools are available to aid with image processing, such as the Argus Merge Tool (AMT) and the Argus Stack Tool (AST). AMT allows users to merge or stack images from multiple cameras into panoramic or plan view images to allow for quantitative measurements. The tool also enables users to rectify images from a single camera. AST was specifically designed for the analysis of bar morphodynamics. AST measures image intensities along user-specific parameters, allowing users to analyze the evolution of the wave breaking patterns over time and quantify bar migration.

Video monitoring systems are often mired by limited storage and management capabilities (Holman and Stanley, 2007). Argus sampling methods have been modified to reduce the quantity of returned data. Those modifications include the production of single-image products that represent the bulk of statistics collected over an entire sampling period (Holman and Stanley, 2007). Most nearshore applications do not require the full sampling capabilities of video cameras and therefore data collection can be downscaled to approximately 2 Hz sampling with a 5m resolution (Holman and Haller, 2013) Downscaling reduces the data rate and enables the user to extend the study duration and expand the spatial coverage (Holman and Haller, 2013). This reduced sampling design is the most employed (and accepted) method among coastal researchers studying nearshore bar systems (Holman and Haller, 2013; Ribas et al., 2010).

3.2.2 Surfcams

Argus stations and other *in situ* coastal imaging systems are site limited because of high operational expenses and installation restrictions requiring a high elevation beach-front or purpose-built tower (Bracs et al., 2016; Brignone et al., 2012). Recreational surf cameras, or surfcams, are a lower cost alternative source of digital images that can be used to study and

monitor nearshore bar systems. Surfcams broadcast near-continuous video streams of beach conditions extending up to several kilometers along the coastline over the internet. While surfcams are relatively new to the study bar morphodynamics, for years, they have proved useful for the integration of research and coastal zone management practices (Davidson et al., 2007; Kroon et al., 2007; Mole et al., 2013; Turner et al., 2006). The data obtained from these systems are used to identify and quantify a diverse range of coastal processes (Kroon et al., 2007; Mole et al., 2013; Turner et al., 2006).

The surfcam stations typically consist of a single robotic pan-tilt-zoom camera mounted on a fixed position that is rotated between pre-programmed aim points (Bracs et al., 2016). Through robotic movements, a single surfcam achieves a similar 180-degree spatial coverage to the Argus system or other fixed camera systems. Surfcams can be inexpensive and less intrusive (compared to Argus) in the coastal setting, since new infrastructure is not required (Bracs et al., 2016; Mole et al., 2013; Turner et al., 2006). Surfcam hardware specifications vary depending on the camera model. For example, CoastalCOMS operates a surfcam network that includes 80 cameras around Australia. The cameras have pan range of 340°, tilt of 115°, and a 26X optical zoom with a specified reposition accuracy of ±0.064° (Bracs et al., 2016; Mole et al., 2013). Surfcams are typically mounted to a low beachfront building and pointed toward the oncoming waves with elevations ranging from 9 to 20m above mean sea level (Bracs et al., 2016; Mole et al., 2013). Low-angle surfcams can present a challenge for shoreline measurement, as the shoreline can be obscured by features in the foreground (Bracs et al., 2016; Brignone et al., 2012; Schiaffino et al., 2013). This means that not all surfcams currently in use are useful for bar identification.

Surfcam videos also can be time averaged to produce timex-like products capturing nearshore images that reveal bar locations. Bracs et al. (2016) conducted an 18-month comparative study between a surfcam and Argus in Australia. The results demonstrated that the mean horizontal errors were approximately 1 m and the standard deviation of error was <2 m by utilizing elevation and rectification methodologies with both systems (Bracs et al., 2016). When comparing the results obtained from the surfcam imagery with monthly real-time kinematic global navigation satellite system surveys from the same locations, the surfcam images horizontal errors were less than 1m (Bracs et al., 2016).

Development of low-cost, easily accessible monitoring systems can address the spatial data scarcity of short- to long-term bar morphodynamics. Surfcams represent a promising source for regional and national coastal and nearshore monitoring programs, but there are limited academic examples that use this technology for nearshore bar identification (Bracs et al., 2016; Mole et al., 2013; Turner et al., 2006). A major limitation of surfcams is that most of these systems do not store data over long periods of time. These video cameras re-write over their data approximately every 2 weeks. Increased partnerships between academia, local governments, and coastal residents and businesses would allow the expansion the surfcam network for nearshore bar monitoring and could help overcome the limitations associated to this system.

3.2.3 Bar identification from video monitoring systems

Identifying bars from images obtained using video monitoring systems has added tremendous value toward understanding bar dynamics. The use of video monitoring systems for nearshore research has led to the development of innovative algorithms and methods that have been employed for the quantitative extraction of geophysical signals from image data

providing new insights of nearshore bar morphodynamics (Alexander and Holman, 2004; Davidson et al., 2007; Gallagher et al., 1998; Holman and Haller, 2013; Alexander and Holman, 2004; Lippmann and Holman, 1989; Plant and Holman, 1998; Ruessink et al., 2002; Thorton et al., 1996). Once the images are normalized and the bars are confidently identified, the bar and surrounding characteristics should be quantified.

The aforementioned algorithms and methods were all created to be employed in Argus environments, but recent studies have demonstrated that they can also be applied to surfcam derived imagery (Bracs et al., 2016; Brignone et al., 2012; Schiaffino et al., 2013). Several tools have been developed for this task (c.f. Alexander and Holman, 2004; Armaroli et al., 2006; Armaroli and Ciavola, 2011; Brignone et al., 2012; Kingston et al., 2000; Madsen and Plant, 2001; van Dongeren et al., 2008). Each tool offers different outputs that benefit our understanding of bar and nearshore morphodynamics, described below (Table 2.1).

Table 2.1 Accuracy assessments from previous studies inferring nearshore bar location.

Reference	Location	Instrument	Method	Accuracy	Error
			Video Monitoring		
Aarninkhof et al. (2000)	Egmond, NLD	Argus	Mapping mult. waterlines per tidal cycle	RMS=0.25m (detection model) RMS=0.10m (elevation model)	σ=0.25 m
Alexander & Holman (2004)	Noordwijk, NLD Duck, NC, USA Palm Beach, USA	Argus	None listed	2.5m	2-21%

Armaroli et al. (2006)	Lido di Dante, Ravenna, ITA	Argus	L-BAIT	r^2=0.4132, 95% significance	+/- 8-10m
Bracs et al. (2016)	9 sites in AUS	CoastalCOMS	None listed	4-20m	4-14m (stdv. error)
Brignone et al. (2012)	Mar del Plata, ARG	Argus	Beachkeeper *plus*	0.16-2.25m	2.1m, σ=1.15
	Pietra Ligure, ITA			0.55-2.90m	2.75m, σ=1.0
Kingston et al. (2000)	Egmond, NLD	Argus	Artificial Neural Network	r^2 =0.87 r^2 =0.77	5m (outer bar) 10m (inner bar)
Lippmann & Holman (1990)	Duck, NC, USA	Argus	Morphologic classification criteria and EOF	15m	5-10%
Madsen & Plant (2001)	Duck, NC, USA	Argus	Modified SLIM	0.1m	Explained 30-40% variance
Plant & Holman (1998)	Duck, NC, USA	Argus	SLIM	0.5m	10%
Ribas et al. (2010)	La Baceloneta & Bogatell Barcelona, ESP	Argus	Induced barline variability	$0.75<H_{rms}<1.5$m $0.5<H_{rms}<1.25$m	+/- 14m +/- 11m
van Dongeren et al. (2008)	Duck, NC, USA Egmond, NLD	Argus	Beach Wizard	0.3m 0.5m	+/- 1 σ

Satellite Imagery

Dehouck et al. (2009)	Truc Vert Beach, FRA	SPOT-4 & 5; FORMOSAT-2	None listed	0.5m	15%
Lafon et al. (2004)	Arcachon Bay, FRA	SPOT	None listed	RMS = 30m	20%
Rodz-Matín & Rodz-Santaella (2013)	Ebro Delta, ESP	ASTER	None listed	RMS = 0.47-0.59	3-8m (derv from geo correction)

Kingston et al. (2000) used an Artificial Neural Network (ANN) to model the cross-shore movement of the Argus timex intensity maximum. Generally, ANNs are a framework for representing non-linear mappings between multi-dimensional spaces governed by several adjustable parameters, specifically in this case, wave climate and water level (Kingston et al., 2000).This technique is applied to reduce the deviations in bar location produced by modulations of the breakpoint by the tide and variations in the incident wave energy (Kingston et al., 2000; López et al., 2017; Ribas et al., 2010). The ANN produces a model for the outer and inner bar systems that allows for the estimation of the cross-shore bar location from the raw Argus image intensity interpolation. However, video-image inferred bar location derived from other methodologies may result in errors up to 30-40m (Kingston et al., 2000; Masselink et al., 2014). The residual errors for the ANN models at a study site in Egmond aan Zee, the Netherlands were <5m for the outer bar and <10m for the inner bar. The R^2 correlation values between ANN estimates and the actual location of the bars were 0.87 (outer) and 0.77 (inner) (Kingston et al., 2000). Several studies have employed ANN

models to gap-fill data sets for periods with no direct measurements and to successfully estimate bar location (Boak and Turner, 2005; Kingston et al., 2000; Plant et al., 2007; Ruessink et al., 2002). It is suggested that ANN is the best current available method for bar extraction (Plant et al., 2007; Ribas et al., 2010).

Alexander and Holman (2004) also developed a process to identify bars from an Argus timex image. After minimizing the noise in the data, they convolved a series of Gaussian functions of varying standard deviations with cross-shore intensity profiles at each longshore location (c.f., Alexander and Holman, 2004). The set of convolutions was summed over a range of standard deviations to estimate energy at each cross-shore location. Bars were identified as peaks within the estimated energy (c.f., Alexander and Holman, 2004). This method requires quality control since non-relevant features, such as piers, create false peaks that could be incorrectly identified as bars (Alexander and Holman, 2004). To find bar locations, Alexander and Holman (2004) also developed a method to normalize bar position based on the tidal level, which reduces tidal bias within the data set. Their method provides an objective differentiation between gaps in the bars (i.e., rip current channels) and errors that arise in the dataset due to lack of wave breaking over offshore features.

The longshore Bar Amplitude Identifier (L-BAIT) was developed to calculate bar crest wave amplitude and length. This tool was formulated by Armaroli et al. (2006) specifically for their study site in Lido di Dante, Italy where there is a tidal range between 0-2 m and $H_{rms} \leq 1.5$m (Armaroli and Ciavola, 2011; Senechal et al., 2015; Tatui et al., 2016). L-BAIT extracts the luminosity peak of 55 pixels of the processed timex image, which creates a matrix for each image with the cross-shore and longshore locations of the bar crest (see Armaroli et al., 2006; Armaroli and Ciavola, 2011). This tool allows users to reject

erroneous luminosity peak positions. It also removes the obliquity of the image due to orientation of the Argus video system axes by rotating and translating them to horizontal axes (Armaroli and Ciavola, 2011). A comparison of bar morphology is possible using L-BAIT because of an imbedded cross correlation function. This method has an accuracy of +/- 8 to 10m and has been tested in other sites with small tidal ranges, such as Biscarrosse, France and Romanian Black Sea Coast (Senechal et al., 2015; Tatui et al., 2016).

Plant and Holman (1997) developed the Shoreline Intensity Maximum (SLIM) method to identify peaks in pixel intensities associated with breaking waves. This method uses the position of maximum perturbation of the actual nearshore profile with respect to a long-term averaged barless profile. The accuracy of this technique to make measurements of nearshore bars depends on the ratio of the measurement errors to the spatial or temporal variability of the beach (Plant and Holman, 1997). Therefore, if the variability of the beach increases, the error of the measurement also increases. Madsen and Plant (2001) modified SLIM by fitting a superposition of quadratic and Gaussian-shaped functions to intensities (i.e., higher pixel values) along a cross-shore transect that included the intertidal and breaking bar zone (Guedes et al., 2011). This method explains 30-40% of the observed slope change variance. The method was deemed sufficiently accurate to characterize beach slope dynamics, since the prediction error variance was equal to, or only slightly lower than, the observed temporal variability of the slopes (Madsen and Plant, 2001). However, this model cannot be used to predict the temporal variability of slopes, since its predictive capability does not outperform models that predict a constant, mean slope (Bapentire at al., 2017; Guedes et al., 2011; Madsen and Plant, 2001).

Beach Wizard is a data assimilation method used to estimate the nearshore subtidal bathymetry based on video-derived observations of wave dissipation and variations of the intertidal shoreline (van Dongeren et al., 2008). Beach Wizard can also be used on radar-derived observations of wave celerity. This method produces estimates of uncertainties in bathymetry, which reflects the sensitivity of the data and true bathymetric evolution (van Dongeren et al., 2008). Beach Wizard employs an inverse model with fewer free parameters, incorporates wave celerity, and reduces the overall error to 0.3-0.5m (rms) (van Dongeren et al., 2008). Simulations show that Beach Wizard-predicted bathymetry falls within +/- one standard deviation of the *in situ* measured bathymetry. Multiple studies concluded that the model is capable of accurately predicting the bar bathymetry for short- and long-term temporal changes (Bergsma et al., 2016; Monteys et al., 2015; van Dongeren et al., 2008). However, Beach Wizard is limited because several estimations must be made during the model set-up phase (van Dongeren et al., 2008). These estimations of bathymetry and wave celerity, if erroneous, can significantly and negatively impact model results.

Beachkeeper *plus* is an open source data fusion based analysis system that integrates timex, variance, time-stacked images, and geo-rectified images to quantify beach morphodynamics (Brignone et al., 2012). It uses the regularization theory to estimate the Direct Linear Transformation (DLT) coefficients in the geo-rectification process without the need to have detailed knowledge on the acquisition system, while reducing errors caused by camera distortion effects (Brignone et al., 2012; Simarro et al., 2017).

3.2.4 Potential sources of error

Images collected from video monitoring are prone to distortion and therefore the user is required to transform image coordinates to real world coordinates, similar to the geo-

rectification process of still-camera imagery. The relationship between image and real world coordinates has been well established and embedded in the Argus video system (c.f., Holland et al., 1997). For example, prior to installation, a camera parameter calibration occurs in the lab. Some parameters, such as tilt, azimuth and roll, depend on installation and need to be included in the post- measurement algorithms used for geo-rectification (Holman et al., 2003). Camera parameter calibration in surfcam systems prior to installation is more difficult since for most situations these cameras are deployed for other purposes for scientific research. In these cases, the user needs to identify the camera parameters and include the necessary calibrations during post-processing.

Camera movement in video monitoring systems associated with rotation during recordings or inconsistent repositioning through time potentially limits data reliability. Error is reduced when fixed cameras are used because the field of view of the camera is least likely to get affected by factors such as strong winds and thermal expansion of the mount (Bracs et al., 2016; Holman and Stanley, 2007; Plant et al., 2007). The methods of data extraction, discussed in section 3.2.3, can isolate signals from noise that allows scientists to clean the images to retrieve reliable and accurate data. These methods are based on the assumption that the processes and variables that affect the signal can be separated by time or space to obtain accurate and reliable bathymetry data (Holman and Haller, 2013).

3.3 Satellite imagery

In the last decade, satellite remote sensors capable of mapping and measuring coastal systems and their changes at high spatial resolutions have been developed to help minimize the need for extensive, but spatially restrictive, field measurements (Dehouck et al., 2009; Holman and Haller, 2013; Klemas, 2011; Teodoro, 2016). The availability of high-resolution

satellites such as IKONOS, QuickBird, and World View, have renewed interest in applying optical remote sensing techniques to the acquisition of bathymetric information in shallow coastal areas due to their high spatial resolution (see Table 2.1) and enhanced water penetration capabilities (Dehouck et al., 2009; Klemas, 2011). Satellite remote sensors have global coverage supported by national and international agencies. High-resolution satellite imagery (Figure 1F) can also provide a more systematic perspective of the bar morphodynamics compared to near Earth imagery, however high resolution satellite imagery lacks the temporal frequency afforded by near Earth imagery (Lafon et al., 2004). Previous work in marine optics demonstrated that high-resolution satellite imagery is an efficient means to map shallow water bathymetry (Dehouck et al., 2009; Lafon et al., 2004, 2002; Lee et al., 1999). This previous work can also be parlayed to extract bar systems using satellite imagery, which can cover study sites with high spatial resolutions (Table 2.1) over several kilometers alongshore (Dehouck et al., 2009).

The sensor type used to identify bar morphodynamics will vary depending on the spectral and radiometric resolution (Klemas, 2011). Spectral resolution is a measure of specific wavelength intervals that a sensor can record, while radiometric resolution is defined as a measure of the ability of a sensor to distinguish between two objects of similar reflectance values (Klemas, 2011). To use satellite imagery for coastal applications, such as bar identification, radiometric calibration of the spectral bands of the sensor has to be robust, since the reflectance of the ocean's surface does not exceed a very small portion of the total signal measured by the satellite sensor (Dehouck et al., 2009; Table 2.1).

To obtain bar morphology from satellite imagery, many characteristics need to be met. Among those characteristics, the study site needs to have relatively clear water so the

bottom is visible (Dehouck et al., 2009). Images must be collected during periods of low wave energy to reduce noise in the data caused by wave breaking (Dehouck et al., 2009; Rodríguez-Martín and Rodríguez-Santalla, 2013). Satellites also have limited to no dwell capability, limiting the spatial coverage of the study site (Holman and Haller, 2013). Dwell time refers to the time a satellite remains steady over one part of the globe. Limited dwell also means that it is incredibly difficult to obtain a significant number of images for a particular location for a fix temporal scale (Rodríguez-Martín and Rodríguez-Santalla, 2013). Atmospheric corrections have to be extremely accurate in coastal environments because water turbidity can make pixel identification un-reliable (Dehouck et al., 2009; Siegel et al., 2000); however obtaining accurate atmospheric corrections is often challenging. Atmospheric correction schemes need to be fully developed, validated and, if required, improved by obtaining *in situ* atmospheric measurements (Dehouck et al., 2009; Holman and Haller, 2013; Monteys et al., 2015).

Errors in the data are introduced through the process of collection, classification, and interpretation and are propagated thereafter (Heuvelink, 2005). Satellite imagery can be modified using enhancing techniques, such as atmospheric corrections, to improve the image quality prior to second order analysis. However, these enhancing techniques can also add errors to the calculations that need to be taken into consideration in the cumulative errors of the analysis techniques. *In situ* data are often used, but not required, to validate and calibrate satellite-derived products (Dehouck et al., 2009; Lafon et al., 2004; Monteys et al., 2015).

Satellite imagery is a valid tool to obtain bar morphology despite the limitations discussed above (Dehouck et al., 2009). While satellite imagery can be used to study bar morphodynamics (i.e., alongshore movements), there are still limitations regarding the

temporal and sampling capacity of the sensors. Increasing these would help researchers calculate bar cross-shore movement and couple it with alongshore movement (Lafon et al., 2004). Future, nearshore bar research would also benefit from the larger spatial scale provided by satellite sensors to study entire systems instead of being restricted to an area of interest within their study site. Satellite imagery provides a global scale, which allows the study nearshore bar systems in locations that were previously not possible due to study site restrictions or equipment lack of availability.

4 Concluding Remarks

It is clear that nearshore bars are complex systems and their study presents a challenge to researchers. One such challenge is that bar systems, similar to all coastal systems and dynamics, are site specific and time dependent. The methods or techniques used to collect data on bar systems, such as beach slope, wave height, tidal range, and bar position and morphology, vary depending on the study site. However, the resultant analysis of these observations made at each site allows for the development of a set of principles that govern holistic bar evolution. This review was prompted by the necessity to synthesize the wide variety of remotely sensed methods and techniques that have been developed to study nearshore bar morphodynamics.

We demonstrated that video monitoring systems are the most popular method for remotely studying nearshore bars. These systems generate multiple deliverables (i.e., timex, long-time variance exposures and single snapshots) that allow for a comprehensive study and understanding of these dynamic regions. Lippmann and Holman's (1989) pioneering video monitoring work continues to be the cornerstone of nearshore bar studies. Their method for extracting nearshore bar morphology has since been modified by through subsequent

contributions (e.g., Kingston et al., 2000; Masselink et al., 2014; Plant and Holman, 1997; and Ribas et al., 2010), but the original technique continues to be recognized as one of the most reliable.

Although video monitoring is the preferred method for bar studies, it is becoming increasingly more common to employ satellite imagery. Satellite imagery has proven to be a useful tool for predicting nearshore bar locations, particularly when it used in conjunction with other datasets (i.e., sonar bathymetry estimates, wave climate data, and tide information). Reasonable estimations of water depth and bar location have been predicted using spatial prediction models, which require satellite imagery (Table 2.1; Dehouck et al., 2009; Lafon et al., 2004; Rodríguez-Martín and Rodríguez-Santalla, 2013). Relatively recent satellite launches of more sophisticated sensors (Landsat-8 and SPOT 6 & 7) provide optimism for continued and lasting advances for the study of bars. These newer sensors have increased capabilities to study bar systems and the coastal zone and will therefore further the scientific understanding of these systems. The major challenge is to have satellite remote sensing techniques adopted as the routine tool in the assessment of the coastal zone. In order to do so, continuous research into the techniques employed for assessing change in the coastal environment is required and the elimination of the degree of uncertainty in some procedures should be a priority (Teodoro, 2016).

Nearshore bars play a pivotal role in coastal dynamics. They are an important source of sediment of the beach-dune system and protect the shoreline from erosion by attenuating wave energy, yet we still lack a thorough understanding of the processes that control their formation and evolution. Remote sensing technologies have significantly advanced our potential to study bar evolution, morphology, and their response to events. Future studies

should further explore the application of surfcams and the adaptation of known Argus methods identification bar systems. This would expand the spatial coverage and reduce the cost of nearshore bar morphodynamic data currently available. Forthcoming studies should also consider satellite remote sensing to study bar systems. Satellite-based sensors provide an extensive and non-invasive perspective of bar systems allowing researchers to holistically investigate entire systems at one time and opening up isolated coastal areas for study. Ideally, the technology will continue to advance, increasing the acquisition and integration of remotely sensed data, which will lead to a more comprehensive perspective of nearshore bar formation and morphodynamics.

CHAPTER 3

APPLYING RULE-BASED CLASSIFICATION FOR NEARSHORE BAR IDENTIFICATION[1]

[1]Román-Rivera, M.A., Ellis, J.T. & Wang, C. To be submitted to *Journal of Applied Remote Sensing.*

1 Introduction

1.1 Nearshore Bars

The nearshore is the transition zone between the land and continental shelf and is significantly influenced by waves during normal and extreme conditions. This area is in constant evolution and its bathymetry varies extensively both temporally and spatially. Some coasts are characterized by sand structures called nearshore bars, which are significant reservoirs of sand. Their position and variability modify the response of beaches to different wave conditions that also influence long- and short-term beach-dune stability (Lippmann and Holman, 1990; Splinter et al., 2011).

Nearshore bars (Figure 3.1) vary in size, from 0.25 to 4.00m high (measured from the seabed to the bar crest), and from 25 to 50m wide, and are found in the inner shoreface aligned parallel (i.e. longshore or crescentic) or slightly perpendicular to the shore (i.e. transverse) (Davidson-Arnott, 2013; Dolan and Dean, 1985; Greenwood and Davidson-Arnott, 1979; Masselink et al., 2011; Wijnberg and Kroon, 2002). Nearshore bars commonly have an asymmetric profile with a gentle seaward slope, a rounded or flat crest, and a steep landward slope (Davidson-Arnott, 2013; Wijnberg and Kroon, 2002). Water depth, swash processes, and currents induced by tidal range differences influence nearshore bar location (Wijnberg and Kroon, 2002). Nearshore bars exist under a wide range of hydrodynamic regimes, from swell- to storm-dominated wave environments and from micro- to macrotidal regimes (Wijnberg and Kroon, 2002).

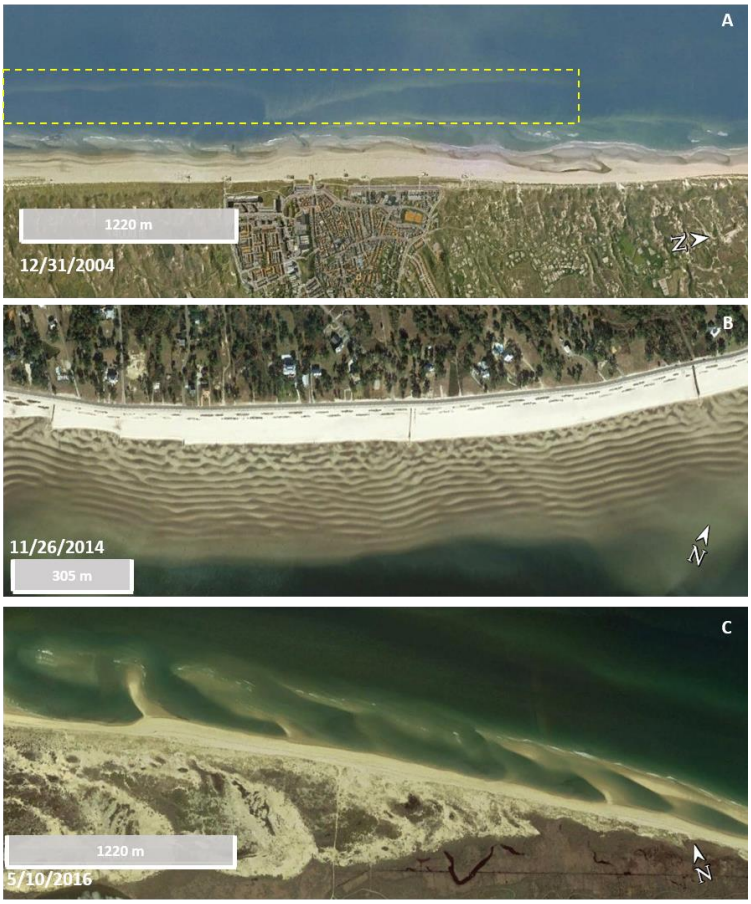

Figure 3.1 Common nearshore bar morphologies. (A) the dashed box shows a crescentic bar in Egmond ann Zee, The Netherlands; (B) depicts a field of longshore bars at Bay St. Louis, Mississippi, USA; (C) illustrates several transverse bars at Cape Cod, Massachusetts, USA. All images were obtained from Google Earth.

The number of bars at a particular location varies depending on nearshore slope. On barred coasts with moderately steep slopes, one to three bars are typically present (Figure 3.1A), while on beaches with gentle slopes, the number of bars can exceed 10 (Figure 3.1B) (Davidson-Arnott, 2013; Greenwood and Davidson-Arnott, 1979; Short and Aagaard, 1993; Wijnberg and Kroon, 2002). A variety of bar configurations are found globally, with the most common ones being transverse (Figure 3.1C), crescentic (Figure 3.1A), and longshore bars (Figure 3.1B).

1.2 Traditional Methods for Monitoring Nearshore Bar Systems

Field-based experiments in the nearshore are often temporally and spatially limited due to the harsh conditions and the high cost of *in situ* instrumentation. Among the limitations that hinder field-based experiments are: instrument failure caused by breaking waves and dangerous currents, substantial erosion or accretion over short periods of time that may scour or bury traditional bottom-mounted sensors, and/or water-level changes related to tidal fluctuations at the study site that can change the fixed sensor's domain range (Holman and Haller, 2013; Lippmann and Holman, 1989). The use of remote sensing technologies permits data gathering in regions that are not easily accessible (Román-Rivera and Ellis, 2019). Specifically regarding this study using multispectral imagery is beneficial in regions that have nearshore bars present but do not have the ideal conditions necessary required for an *in situ* study (Holland et al., 1997; Holman and Haller, 2013; Román-Rivera and Ellis, 2019).

Active and passive remotely sensed instruments, such as radars, light detecting and ranging systems (Lidar), and video monitoring systems, have been employed to study nearshore bar systems (Aleman et al., 2017, 2011; McNinch, 2007; Ruessink et al., 2002). Remote sensing instruments used to monitor nearshore bars must have ample temporal frequency and duration to establish differences between short- and long-term evolution of bar systems (Bracs et al., 2016; Lippmann and Holman, 1990). Any method used to study nearshore bars, regardless if remotely sensed or not, must satisfy the following criteria: a) the shape of the bar must be easily identifiable; b) the position of the crest must be observable; and c) observations must be possible across a range of hydrodynamic conditions (Lippmann and Holman, 1990).

Coastal video monitoring systems are currently the preferred method used to study nearshore bar morphodynamics. The Argus station, for example, is the most frequently used

monitoring system. Argus was developed by the Coastal Imaging Lab (CIL) at Oregon State University, USA. The purpose of this system is to provide a low-cost sampling method to measure the hydrodynamic forcings and the corresponding bathymetric responses of nearshore environments (Holman and Stanley, 2007). The Argus coastal imaging system has collected imagery for almost three decades and has evolved to meet a range of research and management needs. Over time other video systems have been developed based on the Argus utilities and software (i.e. Cam-Era, Kosta System, CostalCOMS, and Horus), but Argus continues to be the most used video monitoring system by the scientific community and by coastal managers (Bracs et al., 2016; Nieto et al., 2010; Splinter et al., 2018). At the time of manuscript submission there are approximately 50 operational sites found in Australia, Brazil, England, Italy, the Netherlands, New Zealand, Japan, Spain, and the United States (see Román-Rivera and Ellis, 2019 and references therein).

Even though coastal video monitoring systems have proven to be a valuable tool to study nearshore bar systems and to provide a wealth of data on bar formation, evolution, and characteristics, they still are subject to a variety of limitations. The limited field of view, making it virtually impossible for researchers to study bar systems that can extend for tens to hundreds of kilometers depending their location and if they are single or multiple bar systems (Davidson-Arnott, 2013; Lippmann and Holman, 1990; Wijnberg and Kroon, 2002). Video monitoring systems, such as Argus, require an *in situ* infrastructure that is dependent on maintenance and is susceptible to damage by severe weather (i.e. hurricanes and/or severe thunderstorms, and erosion) and, in some instances, vandalism. Video monitoring systems also cannot be installed in places difficult to reach, leaving those sites not accessible for research.

1.3 Satellite Imagery and Nearshore Bars

Over the last quarter of the century, satellite remote sensing has been applied to map and measure coastal systems with reduced need for extensive field measurements (Dehouck et al., 2009; Holman and Haller, 2013; Klemas, 2011). Previous work in marine optics demonstrated that high-resolution satellite imagery provides and efficient mean to map shallow water bathymetry (Dehouck et al., 2009; Lafon et al., 2004, 2002; Lee et al., 1999). These study findings can be used to extract nearshore bar systems using satellite imagery, which can cover study sites at a few meter resolution over several kilometers alongshore.

The use of satellite imagery has provided promising results of alongshore bar movements (Ranasinghe et al., 2004.; Ribas et al., 2017, 2010). As discussed in Chapter 2, as technology improves and the temporal and spatial resolution of the sensors increases, we will be capable of gathering more precise data regarding bar formation and degradation (Lafon et al., 2004; Román-Rivera and Ellis, 2019). Nearshore bar research has benefited from the finer spatial scale provided by satellite sensors to study entire systems instead of being restricted to an area of interest between 3-6 km within the study site provided by *in situ* instrumentation (Lafon et al., 2002; Rodríguez-Martín and Rodríguez-Santalla, 2013). Satellite imagery also provides a global scale, which allows the study of nearshore bar systems in locations that were previously not possible to access due to site restrictions or equipment availability (Lafon et al., 2002; Rodríguez-Martín and Rodríguez-Santalla, 2013).

Some considerations that should be taken into account when using satellite imagery to obtain bar morphology include selecting a site that has relatively clear water where the seafloor is visible, and must be collected during periods of low wave energy to reduce noise in the data caused by wave breaking (Dehouck et al., 2009; Rodríguez-Martín and

Rodríguez-Santalla, 2013). Acquiring images that fit the aforementioned parameters will allow for a more robust application of the bar criteria discussed in section 1.2. In this sense, the very high-resolution (VHR) satellite imagery provides decent spatial, spectral, and temporal resolution that fits in this requirement. VHR remote sensing images are becoming increasingly available, which offers us an opportunity to advance our understanding of coastal systems such as nearshore bars (Cheng et al., 2015; Ehrlich et al., 2009; Wang et al., 2018).

This study develops a rule-based object-based image analysis (OBIA) approach for bar identification to acquire bar characteristics (i.e. presence or absence of bars, bar morphology, bar count, and offshore distance from wet/dry land) using VHR multispectral imagery. We also compare the accuracy of the nearshore bar characteristics obtained from the multispectral imagery to those characteristics derived from the traditional Argus video monitoring system. The approach introduced in this study is transferable to other locations where nearshore bars are present. This manuscript focuses on the development, application, and verification of this rule-based OBIA approach for nearshore bar identification. Discussions on the morphodynamics of the bars are beyond the scope of this manuscript.

1.4 Study Area

To develop a comprehensive approach to identifying nearshore bar systems in different environments, three study sites (Figure 3.2) were selected according to their beach characteristics. These sites satisfy two criteria: 1) nearshore bar systems have been previously identified in the region and 2) a video monitoring system has previously been in place. The presence of a video monitoring system enables a comparison of the efficacy of identifying nearshore bar characteristics using multispectral imagery. The rule-based OBIA

approach to identify bars was developed and verified at Duck, NC and Cassino Beach, BRA. After the approach was verified it was implemented at Bay St. Louis, MS, which is characterized by a well-developed multibar system. The selected sites all have a microtidal regime (tidal range <2 m) are:

A. *Duck, North Carolina, USA* (intermediate beach state): The United States Corps of Engineers Field Research Facility for the Coastal and Hydraulics Laboratory in Duck, North Carolina was one of the first Argus locations. The Argus system at Duck has eight cameras that have been operational since October 1986. The breakthrough research using video monitoring systems to monitor nearshore bars was conducted at this site (Lippmann and Holman, 1989). This site has an average wave height of 0.5-2.0 m and an average wave period between 8.0-10 s.

B. *Cassino Beach, Rio Grande do Sul, BRA* (dissipative beach state): This Brazilian beach is characterized by coastal dynamics similar to those found on the west coast of the United States with 1-2 bars present at a particular time. An Argus video monitoring system was installed at this site in 2006 and it acquired data until 2014. Although Cassino Beach and Bay St. Louis are both dissipative beaches, their wave climate conditions are substantially different. Cassino Beach's average wave heights are 1.0-1.5 m, with periods averaging 6.0-12.0 s.

C. *Bay St. Louis, Mississippi, USA* (dissipative beach state): A well-developed bar system is located at Bay St. Louis, Mississippi. The United States Naval Research Laboratory at NASA Stennis Space Center oversees the Argus tower at the Washington Street Pier. These data are available from 2002-2005. Bay St. Louis has an average wave height of 0.3-1.0 m and average wave period of 0.5-3.0 s.

Figure 3.2 The three study sites: A) Duck, NC; B) Bay St. Louis, MS; C) Cassino Beach, RS; D) Location of nearshore bar systems. The yellow triangle ( ) identifies the location of the Argus tower.

2 Data

2.1 Multispectral Imagery

Two high quality multispectral images at each study sites were obtained from Digital Globe. Digital Globe manages the WorldView satellite series and QuickBird. The imageries acquired were already georectified and atmospherically corrected.

The selected images correspond to years with concurrent Argus Timex data sets and to winter and summer months for Duck, NC and Bay St. Louis, MS to provide two distinct beach state conditions at each site. For Cassino Beach, BRA it was not possible to obtain a suitable winter VHR image that corresponded with Argus imagery due to the high wave energy this coast receives during the winter months. Instead a summer (11/19/2010) and an autumn (02/09/2010) image were acquired. To conduct the rule-based OBIA approach, 4

multispectral bands were used (visual and NIR). The VHR images at each site are listed in Table 3.1.

Table 3.1 VHR images used for this study.

Location	Source	Date	Resolution	
			Spectral	Spatial
Duck, NC	WorldView-3	08/16/2016	RGB, NIR	30 cm
Duck, NC	WorldView-3	02/24/2017	RGB, NIR	30 cm
Cassino Beach, RS	WorldView-2	02/09/2010	RGB, NIR	50 cm
Cassino Beach, RS	WorldView-2	11/19/2010	RGB, NIR	50 cm
Bay St. Louis, MS	QuickBird	02/02/2003	RGB, NIR	60 cm
Bay St. Louis, MS	QuickBird	07/11/2005	RGB, NIR	60 cm

2.2 Argus Data

Argus stations comprise four to five video cameras with a 1024x768 pixel resolution, a field of view that spans 180°, and aim angle within 0.1 pixel or 0.004° (Holman and Stanley, 2007). These parameters allow for a spatial coverage of 3-6 km of the nearshore (Aarninkhof et al., 2000; Bracs et al., 2016; van Enckevort et al., 2004). An Argus system provides a 10-minute time exposure image (or Timex) from the mathematical mean of images collected every 30 seconds (Holman and Stanley, 2007). Timex runs initiate at the top of the hour for 12 (assumed) hours per day. For this study we used the Timex imagery to verify the nearshore bar classification. Timex images are often used to delineate areas of wave breaking and obtained by averaging fluctuations due to incident wave modulations (Lippmann and Holman, 1989; Ribas et al., 2010; van Enckevort et al., 2004). Therefore, these images can be used to calculate the location of bars based on were the waves break as shown in Figure 4.3 within the yellow box.

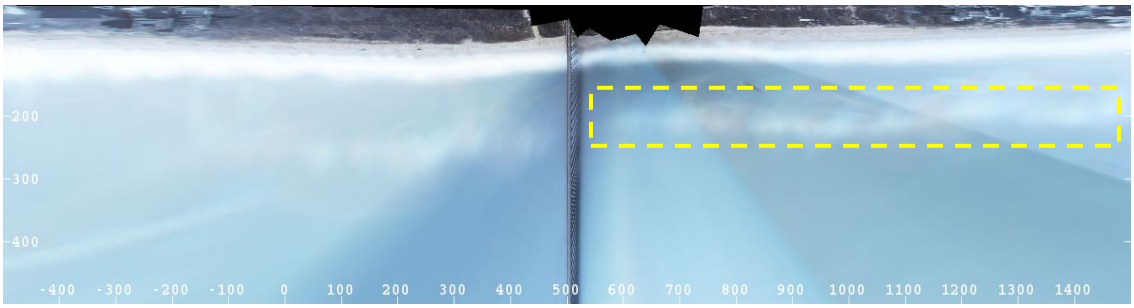

Figure 3.3 Example of a Timex image obtained from the Argus System at the USACE Field Research Facility at Duck, NC. The pier is at the image center and a nearshore bar is within the dashed box. The scale in the image is in meters, depicted with the white number on the image. Imagery date: 02/24/2017.

Argus imagery was obtained from different sources, since the video monitoring systems were maintained by different entities. The Argus Timex imagery for Duck, NC was provided by U.S. Army Engineer Research & Development Center, Coastal & Hydraulics Laboratory, Field Research Facility, Duck, NC. The Timex imagery can be downloaded from the FRF Data Portal (https://frfdataportal.erdc.dren.mil/). Imagery for Bay St. Louis was provided by Dr. K. Todd Holland from the Naval Research Laboratory at the NASA Stennis Space Center. Lastly, Argus Timex imagery for Cassino Beach, RS was provided by Dr. Lauro Calliari from the Federal University of Rio Grande, Brazil.

3 Methodology

3.1 Decision Tree for Shoreline Bar Identification: Preparation and Execution

Decision trees are a multistage classification approach to break up a complex procedure into a union of several simpler decisions. Decision trees are an effective tool due to their conceptual simplicity and computational efficiency.

This study applies an object-based (or objected-oriented) image analysis (OBIA) classifier to identify the nearshore bars at each location. Increased spatial resolution imagery

favors OBIA classification methods over other per-pixel classification analyses because it allows the analyst to look at an object composed of more than one pixel (Blaschke, 2010; Heumann, 2011). In OBIA, groups of pixels are classified into representative shapes and sizes. This process is a multi-resolution segmentation that produces homogenous image objects by grouping pixels based on texture, context, and geometry (Blaschke, 2010; Blaschke et al., 2014; Bouziani et al., 2010; Tarabalka and Tilton, 2012). Each class contains one or more rule that is based on the user's knowledge of a particular feature. The rules may contain one or more attributes such as spectral, spatial or texture, from which the user can assign a specific range of values.

The Feature Extraction Module (ENVI Fx) in ENVI 5.5.1 package (Jahjah and Ulivieri, 2010) was used. ENVI Fx automatizes the extraction of features from high resolution imagery based on spatial, spectral, and textural characteristics (i.e. dimensions of a feature, pixel value, and/or appearance of an object given by its shape, density or arrangement). Salient visual image interpretation cues are quantified for a feature, machine learning components are trained with these cues, and the learned cues are applied to the imagery to derived features. The tool allows the user to customize the spatial, spectral, and textural parameters for extraction of features to a specific application. A summary of the workflow of the module is shown in Figure 3.4.

Step A is to select the base images from which the features will be extracted and prepare them for analysis (Figure 3.4A). A mask was created using ENVI's Build Raster Mask tool to specify the area of interest within the image to confine the processing and to reduce the overall processing time by focusing on the nearshore area that contains the bars. The subaerial beach is not included. The mask matched the Argus camera field of view of

each location and generated a polygon over the VHR multispectral imagery. The extent of the camera field of view was obtained from the results produced from the Argus Timex image produced in Matlab (see section 3.2).

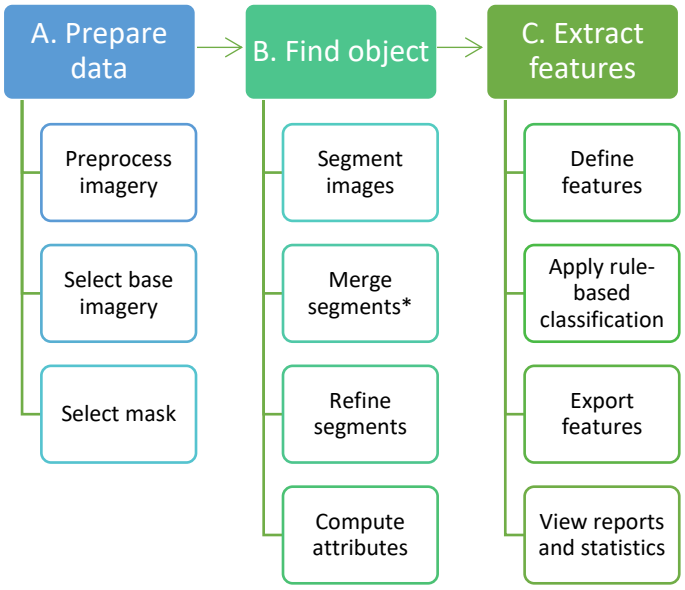

Figure 3.4 Recommended ENVI Fx workflow. This workflow has not been previously applied for nearshore bar extraction. (*) means that this step is optional.

Step B is to locate the objects, i.e. the nearshore bars in this study (Figure 3.4B). First, the images were segmented, which refers to the process of partitioning the image by grouping neighboring pixels with similar feature values together. This partitioning or segmentation takes places by assigning the image a value for Scale Level. The Scale Level value in the ENVI Fx for each location was different since the nearshore bars at each location have different scaling parameters. The Scale Level is computed from a normalized cumulative distribution function of the pixel in the image to effectively delineate the boundaries of the features without over-segmenting the features (Jin, 2012). A proper Scale Level keeps objects with the most distinct edges. The Scale Level values range from 0.0

(finest segmentation) to 100.0 (coarsest segmentation), the lower the Scale Level value, the more segments are going to be defined. During segmentation, spectral, morphological, and spectral attributes are calculated and included in the image classification to avoid noise in the pixel-based classification. The segmentation was completed using an edge-based process. This edge-based process identifies features with distinct boundaries. With this method, ENVI computes a gradient image using a Sobel edge detection method, where the highest pixel values represent areas with the highest pixel contrast. After multiple tests, the Scale Level values used in this study were: Duck, NC: 53.4 and 90.0, Bay St. Louis, MS: 65.0 and 80.0, and Cassino Beach, RS: 50.0 and 53.4.

After defining the segments, merging was necessary to aggregate the small segments within larger textured areas where there was over-segmentation. Over-segmentation occurs where the feature is segmented, in this case the nearshore bars, and fractured into subcomponents. Over-segmentation may increase the chance that important boundaries were extracted, but it does so at the cost of creating insignificant boundaries (Taguchi et al., 2008). The Merge Level parameter in the ENVI Fx represents the threshold lambda value that range from 0.0 to 100.0. The values used for the images were: Duck, NC: 90.0 and 90.7, Bay St. Louis, MS: 42.9 and 88.5, and Cassino Beach, RS: 87.1 and 90.0. Merge Level values were assigned based on visual interpretation. While visual interpretation utilizes the spectral, contextual, and textural information of the imagery to identify the boundaries of the nearshore bars, this may affect the overall results of the feature extraction process by introducing biases to the interpretation (Petit and Lambin, 2001; Shalaby and Tateishi, 2007).

Step C is feature extraction. After segmentation and merging took place, rules were created to identify the bars. The rules applied to identify the bars were based on the average pixel values of a specific band over the bars for each image (Table 3.2). The bars at Duck, NC and Cassino Beach, RS were found deeper in the water column, therefore the green band was used to segment the images at these two locations. At Bay St. Louis, MS, the bars can be found closer to the surface and the NIR band provided a better base for the segmentation process to take place. For the rule-based classification spectral attributes were computed on each band of the input image, including the spectral mean (mean value of the pixels comprising a region in a particular band) and the spectral standard deviation (standard deviation value of the pixels comprising the region of a particular band). The pixel values shown in Table 3.2 were selected based on visual interpretation of the segmented image created.

Table 3.2 Pixel values used for rule-based classification approach. For Duck, NC and Cassino Beach, RS the green band was used to segment the images and acquire pixel values. For Bay St. Louis, MS the NIR band was used.

Location	Date of VHR image acquisition	Pixel Values
Duck, NC, USA	08/16/2016 02/24/2017	151.83-246.50 177.50-248.00
Cassino Beach, RS, BRA	02/09/2010 11/19/2010	99.62-154.08 115.65-154.94
Bay St. Louis, MS, USA	02/02/2003 07/11/2005	113.79-136.73 120.92-163.25

After the bars were classified, the images were exported to ArcGIS where bar width, height, count, and offshore distance were calculated using the Calculate Geometry tool.

3.2 Verification of Satellite-Identified Shoreline Bars

Argus Timex data were obtained at the same location and time as the VHR images are used to verify the classified nearshore bars. Within the Timex images, nearshore bar characteristics are calculated using a Matlab code freely available on the Coastal Imagine Research Network (CIRN) web page (https://coastal-imaging-research-network.github.io/#/). This Matlab code, called cBathy Toolbox, allows bar characteristics, such as count, length, and width to be calculated and extracted from Argus images.

In this study, it is assumed that the Argus-based bar identification extraction method is the standard (or 'truth'). The proposed method is verified in two out of the three locations. The method was implemented at Bay St. Louis, MS. A comparison is completed for two dates at each location to compare the bar systems during different conditions. Bar width, height and count, and distance from the average wet/dry line are compared using a threshold of acceptable error of ≤10% (Lippmann and Holman, 1990, 1989; Ribas et al., 2017). Error was calculated using the formula (Equation 3.1) comparing the measurements acquired using the rule-based OBIA approach and those extracted from the Argus Timex imagery.

$$\%_{error} = \left(\frac{m_R - m_A}{m_A}\right) * 100\ , \tag{1}$$

where m_R represents the measurement obtained from the rule-based OBIA approach and m_A represents the measurement obtained from the Argus Timex imagery (what we consider 'truth'). The percent error formula (equation 1) was the most suitable method for data verification due to the binary nature of the data being extracted. A positive percent error indicates the rule-based OBIA approach is overestimating the measurements compared to Argus. A negative error indicates the rule-based OBIA approach is underestimating the measurements compared to Argus.

4 Results and Discussion

Single nearshore bars systems were successfully identified and characterized at both locations. Bar count, offshore distance of the bar to the wet/dry line, and average length and width of the bars were extracted. After the new approach was verified, the approach was applied to the multiple bar system located at Bay St. Louis, MS. The results for each location are presented and discussed below.

4.1 Rule-Based OBIA Approach Development and Verification

4.1.1 Duck, NC

Duck, NC has a discontinuous single bar (Figure 3.5). The bar morphology varies between a longshore and crescentic bar. In the coastal community, these morphologies are known as rhythmic bars and the changes between the two result from a coupling mechanism between the beach hydrodynamics and bathymetry (see Davidson-Arnott, 2013). The summer image (08/16/2016) presented a longshore bar south of the pier, while the winter image (02/24/2017) identified a bar north of the pier and another one southern of it. The bars identified in the winter were much larger than the single bar identified during the summer. The bar dimensions at Duck, NC are shown on Table 3.3.

When classifying the winter VHR image (02/24/2017), a bar was identified south of the pier. This bar could not be verified using Argus because that portion of the image was over exposed. The VHR measurements shown on Table 3.3 are those obtained from the bar identified north of the pier (Figure 3.5B). This bar presented characteristics of a crescentic bar with an approximate length of 120.74 m and a width of 4.50 m. It was approximately 15 m from the wet/dry line.

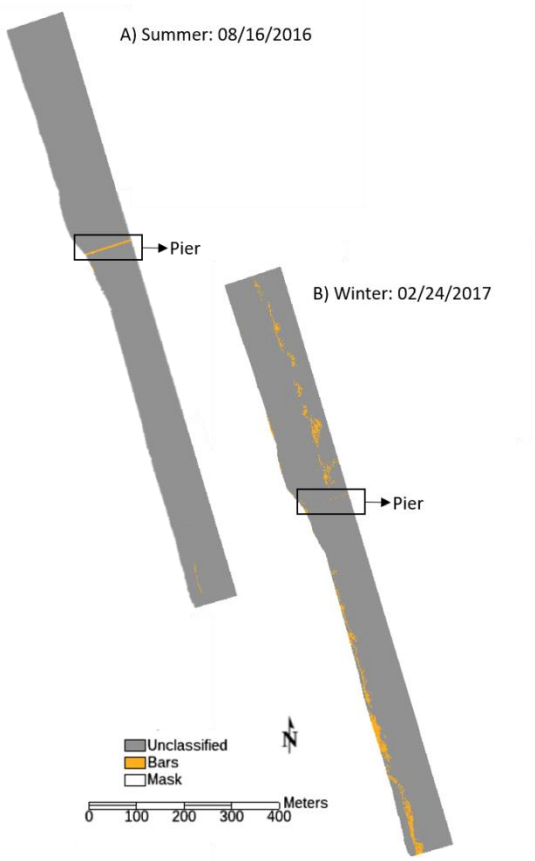

Figure 3.5 Classified bars at Duck, NC. A) 08/16/2016: summer conditions; B) 02/24/2017: winter conditions.

Table 3.3 Bar characteristics at Duck, NC based on imagery from 08/16/2016 and 02/24/2017. The rule-based OBIA approach results use the VHR and the Argus Timex images.

	Study Area (km)	**Bar count**	**Average bar length (m)**	**Average bar width (m)**	**Distance wet/dry line (m)**
08/16/2016					
VHR	1.80	1	106.04	3.55	34.10
Argus	1.80	1	115.26	3.64	37.32
Error			*-8%*	*-2%*	*-9%*
02/24/2017					
VHR	1.80	2	715.25	22.96	107.20
Argus	1.80	1	796.86	24.78	100.14
Error			*-10%*	*-7%*	*7%*

Duck, NC presented interesting challenges for using multispectral imagery for bar identification. The spectral signature for the bars was similar to that of breaking waves, making them difficult to distinguish during the segmentation process. Therefore, it is important to find images with little to no waves breaking and foam near the shoreline. The OBIA approach underestimated the bar dimensions (length and width) but was inconsistent with the estimation of the location (Table 3.3). It underestimated the distance of the bar from the wet/dry line in the summer image (08/16/2016) and overestimated the distance in the winter image (02/24/2017). Overall, the error is still within the acceptable threshold (≤10%), however we posit the high wave energy could have contributed to the higher error percentages when compared to the site at Cassino Beach.

4.1.2 Cassino Beach, BRA

Similar to the Duck site, Cassino Beach is a single bar system (Figure 3.6). The bar found at this location is a nearshore bar. The nearshore bar extends 333.28m in the summer (02/09/2010), while the bar identified later that year during spring (11/19/2010) is shorter with a length of 279.45m. The November bar is substantially narrower (8.02m) than it was nine months earlier (26.11m). Another difference is that the bar in February is located further offshore (51m) than the bar identified in November (13.62m).

The bars at Cassino Beach were easier to identify compared to Duck since the water column at Cassino is clearer and the beach has lower wave energy. The percentage error for the bar characteristics is generally lower than those obtained at Duck and within the <10% error threshold. (Table 3.4). At this location the OBIA approach over-estimated location and exhibited mixed results regarding bar dimensions. VHR imagery results underestimated bar length and width on 02/09/2010 and over-estimated those same parameters on 11/19/2010.

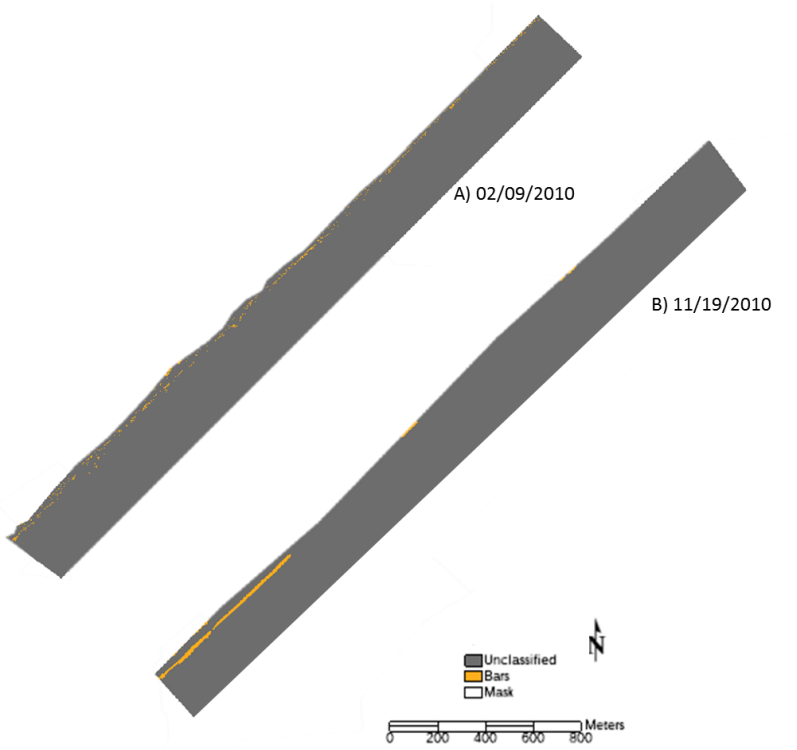

Figure 3.6 Classified bars at Cassino Beach, BRA. A) 02/09/2010; B) 11/19/2010.

Table 3.4 Bar characteristics at Cassino Beach, BRA based on imagery from 02/09/2010 and 11/19/2010. The rule-based OBIA approach results use the VHR and the Argus Timex images.

	Area (km)	**Bar count**	**Average bar length (m)**	**Average bar width (m)**	**Distance wet/dry line (m)**
02/09/2010					
VHR	2.00	1	333.28	26.11	51.00
Argus	2.00	1	340.35	28.46	47.53
Error			*-2%*	*-8%*	*7%*
11/19/2010					
VHR	2.00	1	279.45	8.02	13.62
Argus	2.00	1	270.64	7.64	12.86
Error			*3%*	*5%*	*6%*

4.2 Rule-Based OBIA Approach Implementation: Bay St. Louis, MS

After verifying the results of the rule-based OBIA identified nearshore bars using VHR images at Duck, NC and Cassino Beach, RS, we implemented the approach at Bay St. Louis, MS to characterize a multiple bar system. The multiple longshore bar system at Bay St. Louis location could clearly be seen after the rule-based OBIA approach was applied to both images at this location (Figure 3.7). The bars closer to the shoreline, in shallower depths, could be identified easier than those bars located further offshore, in deeper water since there was clearer pixel separation between the nearshore bar and sediment suspended in the water. The main challenge with bar identification at this location is the suspended sediment located further offshore surrounding the deeper bars. During image classification, the spectral values for the deeper bars and the suspended sediment are the same, which is a limitation.

The bars at this location tend to be organized in continuous rows 2.0 to 4.0 meters from each other. The width of the bars varies within the images. Wider (8.0 to 12.0 m) bars are present in the western portion of the study site, and thinner (3.0 to 5.0 m) bars are found in the eastern portion of the study area (Table 3.5). The number of bars identified is also higher on the western side of the study area than the eastern, which may have to do with the wave angle of approach. Also, the Washington Pier is located at the western extreme the study site (not shown in Figure 3.7 since the pier was not included in the mask), which disrupts the sediment flow and affects the organization and formation of the surrounding bars.

Table 3.5 Bar characteristics at Bay St. Louis, MS. The rule-based OBIA approach results are shown for 02/02/2003 and 07/11/2005.

Date	Area (km)	Bar count	Average bar length (m)	Average bar width (m)	Distance wet/dry line (m)
02/02/2003	2.00	13	633.39	10.86	6.0
07/11/2005	1.16	12	344.12	4.56	8.0

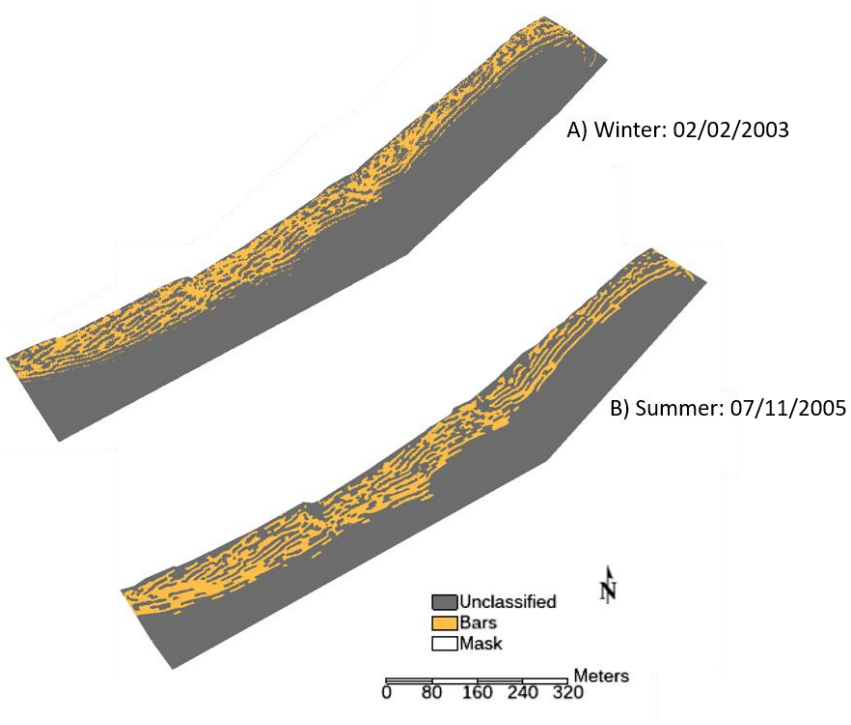

Figure 3.7 Classified bars at Bay St. Louis, MS. A) Winter: 02/02/2003; B) Summer: 07/11/2005.

The bars identified by Argus are located in the same region where the rule-based classification approach cannot distinguish suspended sediment from bars. Therefore, data verification at this location was not possible. Nonetheless, in the previous two sites we demonstrated that the use of the rule-based classification and multispectral imagery provides a wealth of information about the bars at this location, making it possible to study a larger portion of the system than that provided by the video monitoring system. The implementation of the rule-based OBIA approach at Bay St. Louis demonstrates that it can also be used to identify multiple bar systems and can be applied to systems located in Case 2 waters. As discussed above there are some limitations associated to applying the method to

environments with this condition (case 2 waters), specifically related to suspended sediment and clarity of the water column, but identification of bars is still possible.

The application of the rule-based classification to identify nearshore bars at Duck, NC and Cassino Beach, BRA was successful with percent errors of ≤10%. At Duck, NC measurements were underestimated, while at Cassino Beach most measurements were over-estimated. These discrepancies are likely due to the conditions of the sites at these locations at the time the VHR images were obtained. Discrepancies might have also resulted from visual interpretation error during the segmentation and merging process. The application of the approach at Bay St. Louis, MS demonstrates that multispectral imagery can be used to study nearshore bars systems.

Ancillary data can be added during Step A of the feature extraction process (Figure 3.4) to improve the results of the OBIA approach. More data, such as nearshore bar volume and height, could be obtained if ancillary data (i.e. bathymetry), are available to supplement the bar identification process. Bathymetric data will also refine the nearshore bar boundaries, which will improve the results of the rule-based OBIA approach. Unfortunately, temporal coincident bathymetric data were not available for all locations. However, bathymetric data should be used with caution for these types of studies since, in some instances, it is not updated at the same temporal frequency at which nearshore bar systems change.

The limitations associated with this workflow are similar to those associated with any remote sensing study, since very specific image characteristics must be in place to successfully identify the bars. The images must not contain any sun glint, little to no waves or wave foam, and little to no suspended sediment since it affects the segmentation and classification process. Regardless of the limitations, this approach can be applied to

nearshore bar environments, including those systems located in regions were there are no video monitoring systems available. Nearshore bars influence dynamics in of the beach and dune systems (c.f. Davidson-Arnott, 2013). Therefore understanding how nearshore bars evolve and how their changes are related to the beach-dune response are important to create effective coastal management plans and to protect coastal infrastructure and resources. The application of the rule-based OBIA will allow coastal scientists and managers to increase the spatial and temporal capabilities at which they study nearshore bar systems. The use of the approach will also make the acquisition of nearshore bar characteristics accessible at a decreased cost compared to *in situ* projects.

Since the launch of IKONOS in 1999, an increased number of commercial satellites (including small satellites) have been in operation. Their capability of acquiring high-resolution imagery with a large spatial extent and having repeated cycles is superior in continuous observation and characterization of nearshore bars. Future research should focus in applying the rule-based classification approach introduced here to identify nearshore bars can be applied to aerial photography, as well as free online resources such as Google Earth, ArcGIS basemaps, and Bing imagery, for example, and the use of unmanned automated vehicles (UAVs) are opening the doors to lower cost equipment to attain nearshore bar characteristics.

Nearshore bar research can benefit by the larger spatial scale provided by satellite sensors to study the entire coastal system instead of being restricted to a limited area of interest monitored by station-based video systems. Satellite imagery provides a global scale, which allows the study of nearshore bar systems in locations that were previously not possible due to site restrictions or equipment availability.

5 Conclusions

This study develops a rule-based OBIA to identify nearshore bars from VHR imagery and makes an important methodological contribution to nearshore bars research. Rule-based classification OBIA approach allows bar characteristics such as bar length, width, and count, as well as distance from the wet/dry line to be measured. Important implications for coastal scientists and managers emerge from this development since we are now able to obtain these characteristics without being intrusive in the environment, at a lower cost, and in locations that weren't accessible before. The use of VHR imagery will also allow the study of the entire nearshore bar system, which can extend from tens to hundreds of kilometers, and understand how it changes and evolves in its entirety through time instead of observing a fraction of the system as it was previously done with *in situ* studies and with video monitoring systems. The method was verified using Argus Timex imagery at two sites, Duck, NC and Cassino Beach, BRA, and implemented at Bay St. Louis, MS. Single and multiple bar systems with different morphologies were identified and characterized at three locations used in this study.

Using multispectral imagery provides a lower cost alternative to monitor coastal systems, compared to *in situ* studies or to the preferred video monitoring systems (Bracs et al., 2016; Holman and Stanley, 2007; Lippmann and Holman, 1990) since it requires no equipment maintenance. This approach provides the opportunity to study bar systems located in regions that are not accessible for field studies or were infrastructure, such as video monitoring systems, can be mounted.

The field of coastal geomorphology studies the dynamics and processes that occur in coastal regions. The higher spatial and temporal scale capabilities provided by VHR imagery

could provide in the future important information regarding bar evolution. Understanding the spatiotemporal scale at which nearshore bar systems evolve and how those patterns are related to beach-dune response are important to create effective coastal management plans to protect coastal resources and infrastructure in the region. The application of rule-based classification to identify nearshore bars is a novel approach that will increase the spatial and temporal capability to study nearshore bar systems at a decreased cost compared to *in situ* projects. Integrating traditional remote sensing technology to coastal management and studies will increase data accessibility to researchers, managers, and stakeholders in order to better understand, manage and protect our coastlines.

CHAPTER 4

BEACH-DUNE RESPONSES TO HIGH-ENERGY WAVE EVENT CONDITIONS INFLUENCED BY NEARSHORE BAR MORPHOLOGY[1]

---

[1]Román-Rivera, M.A. & Ellis, J.T. To be submitted to *Annals of the Association of American Geographers.*

1 Introduction

The coastal zone is one of the most dynamic geomorphic systems on Earth (Elko and Holman, 2014; Sherman and Bauer, 1993). It possesses natural, commercial, recreational, ecological, and industrial value that is vital to any country (CZMA, 16 U.S.C. § 1451, section 302). This densely populated region is threatened by short- and long-term erosion caused by sea level rise, tropical systems, winter storms, and anthropogenic influences (Clark, 1997; Elko and Holman, 2014; Thia-Eng, 1993). Before the 20th century, most coastal zone and nearshore studies were conducted by engineers and involved the planning, design, and construction of projects aimed at counteracting subsidence, protecting shorelines, facilitating navigation, and building harbors (Orme, 2013). Following the ideas of William Morris Davis, geographical and geomorphological studies related to the evolution of the coast and coastal classifications emerged in the first decade of the 20th century (Bird, 1993; Davidson-Arnott, 2010). It was during this time that geographers got heavily involved in coastal studies (Stephenson and Brander, 2003), an involvement that continues to this day. Geography provides an ideal framework for coastal system studies because it offers the opportunity to establish linkages between morphological changes and processes at intertwining temporal and spatial scales (French and Burningham, 2011; 2013; Jackson et al., 2019). The geographic framework also permits the incorporation of anthropogenic topics to coastal studies by providing knowledge to understand our role in the evolution and development of coastal systems.

Technologic advances in the 1950s allowed coastal geomorphologists to conduct more comprehensive studies of the nearshore, which previously had proven challenging (French and Burningham, 2009; Román-Rivera and Ellis, 2019). The nearshore is a transition zone between the land and the continental shelf that is significantly influenced by waves during normal and extreme conditions. It represents an important and highly active region of the coastal system.

Accordingly, bathymetry in this region varies extensively (Splinter et al., 2011; Wright and Short, 1984).

The nearshore is often dominated by sand bars. Sand bars naturally protect the coast against erosion by dissipating wave energy (Masselink et al., 2011; Short and Hesp, 1982). They are substantial reservoirs of sand, and thus, they may impact the response of beaches to different wave conditions. Bar position and morphologic variability also influence long- and short-term beach and dune stability (Lippmann and Holman, 1990). While interactions between the beach, dune, and bar systems are recognized in the literature (e.g., Bauer, 1991; Houser, 2009; Pye, 1982; Sherman and Bauer, 1993), few studies have investigated the intricacies of the relationships between these features. This research will, therefore, focus on studying the dynamics of the dunes, beach, and, specifically, nearshore bars to understand how these three coastal features systematically function. We follow a holistic approach similar to Short and Hesp (1982) instead of those studying the individual features in isolation (i.e. Bowen, 1980; Houser and Hamilton, 2009; Masselink et al., 2014; Wijnberg and Kroon, 2002).

1.1 Nearshore bars and beach-dune characteristics

Nearshore processes, such as sediment and water movement generated by waves and currents, play an important role in determining the morphodynamic beach state. These processes shape the overall geometry of the foreshore, beach slope, grain distribution, and beach width (Houser and Ellis, 2013; Sherman and Bauer, 1993), which in turn affect and influence dune formation. Nearshore characteristics (i.e., presence or absence of bars, bar count, and slope) regulate sediment delivery to the subaerial beach (Bauer, 1991; Pye, 1982; Sherman and Bauer, 1993). Knowledge of bar morphodynamics can provide a better understanding of the subaerial beach-dune system dynamics. The nearshore morphodynamic system is a direct manifestation of the hydrodynamic and morphodynamic boundary

conditions. These boundary conditions depend on the wave climate, nearshore currents, beach slope and orientation, sediment characteristics, and distribution.

Short and Hesp (1982) provided the benchmark classification of beach-dune system morphologies using the surf zone characteristics of slope, breaker height, presence or absence of bars, and bar morphology. Nearshore characteristics influence the wave height and energy received at the beach. The authors integrated the surf zone and beach characteristics to identify beach states as dissipative, intermediate, and reflective, each with characteristic slopes and erosion rates (Short and Hesp, 1982). Later, the linkages between nearshore processes and beach states were investigated to include near bottom current variabilities (Ruessink and Jeuken, 2002) and wave climate (Wright and Short, 1984). Wright and Short (1984) specifically provided bar characteristics for each Short and Hesp (1982) beach state. The Wright and Short (1984) classification has served as the foundational work for nearshore bar studies and bar classifications schemes, as it was one of the first to offer a holistic view of the relationship between the dune, beach, and bar characteristics (Lippmann and Holman, 1990; Ribas et al., 2010).

In later years, researchers expanded on the linkages between beach-dune dynamics and nearshore dynamics (Davidson-Arnott and Law, 1996; Houser et al., 2008; Wijinberg and Kroon, 2002). Dissipative beaches have a larger *fetch* (defined as the distance over which wind acts; Davidson-Arnott and Law, 1996) that allows for greater sediment to potentially transport across the beach. This beach state is also characterized by well-developed bar systems (Short and Hesp, 1982; Wijinberg and Kroon; 2002; Wright and Short, 1988). Dissipative beaches have a lower frequency of *wave set-up* (an increase in mean water level due to breaking waves) reaching the upper beach and backshore potentially

causing beach erosion and dune scarping (Hesp 1988; Houser and Ellis, 2013; Short and Hesp, 1982). Contrary to dissipative beaches, intermediate beaches have a more variable fetch due to a higher frequency of wave set-up and beach mobility. Intermediate beaches are also characterized by crescentic nearshore bar systems (Figure 4.1C; D).

Reflective beaches typically have a low potential for sediment transport across the backshore due to the acceleration of the wind across the steep beachface followed by a rapid deceleration beyond the crest. At this beach state, potential transport is only possible in locations where the backshore is wide enough to permit the adjustment of the boundary layer (Houser et al, 2008; Houser and Ellis, 2013). Reflective beaches are not considered in this study since they often do not have bars (Hesp, 2012).

1.2 Nearshore bar classifications

Nearshore bars can extend from a few meters to kilometers along the coast. Nearshore bars are relatively large bedforms (0.25 – 4.0 m high, 25 – 150 m wide) found in the inner shoreface and can be aligned slightly perpendicular to the shore (i.e., transverse, Figure 4.1A; B) or parallel, such as crescentic (Figure 4.1C; D) and longshore (Figure 4.1E; F) (Greenwood and Davidson-Arnott, 1979; Davidson-Arnott, 2013; Dolan and Dean, 1985; Masselink et al., 2011; Wijnberg and Kroon, 2002). Water depth, swash processes, and nearshore currents induced by tidal range differences influence their location (Wijnberg and Kroon, 2002). These exist under a wide range of hydrodynamic regimes, from swell- to storm-dominated wave environments and from micro- to macro-tidal ranges (Wijnberg and Kroon, 2002).

Several nearshore bar classifications have been conceptualized (Greenwood and Davidson-Arnott, 1979; Lippmann and Holman, 1990; Wijnberg and Kroon, 2002; Wright

and Short, 1984). Each classification scheme uses different variables (beach state, beach slope, wave climate, tidal range) to differentiate bar types. These classification schemes use site specific spatial and physical characteristics to describe bars. One of the most used bar classification schemes is the 'Australian model' (Wright and Short, 1984). The 'Australian model' is distinctive from previous schemes (e.g., Greenwood and Davidson-Arnott, 1979; Shepard, 1950; Sonu, 1968) because it considers the effect of the beach state (i.e. dissipative, intermediate, or reflective) on bar morphology (Grasso et al., 2009; Price et al., 2011). Another highly cited bar classification is the 'Dutch model' (Ruessink and Kroon, 1994). This model classifies nearshore bars in terms of the bar morphometric parameters, such as crest depth, height, width, and volume (Plant and Holman, 1997; Ruessink and Kroon, 1994).

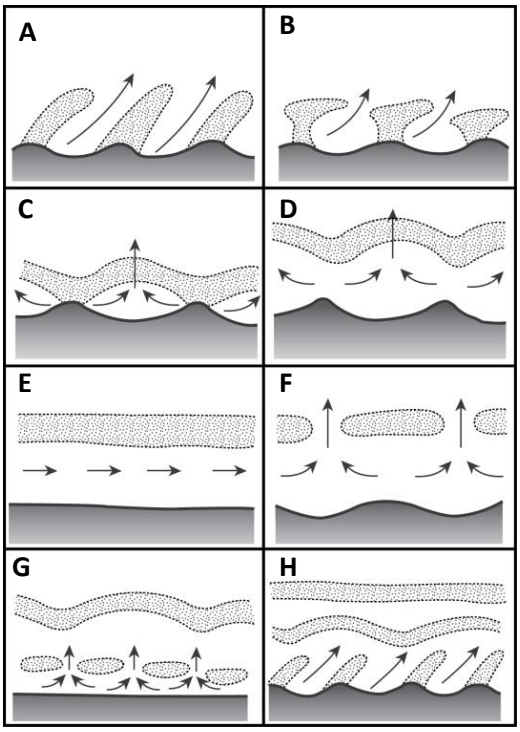

Figure 4.1. The figure illustrates: A) and B) transverse bars; C) shore-attached crescentic bar; D) crescentic bar; E) longshore bar; F) segmented longshore bar; G) double bar system; H) multiple bar system. Arrows indicate the current circulation in the nearshore. Modified from Masselink and Hughes (2003).

Lippmann and Holman (1990) developed the first nearshore bar classification using a video monitoring system. This classification expanded the 'Australian model' classification (Wright and Short, 1984) by adding two additional beach-bar configurations and incorporating the 'Dutch model' (Ruessink and Kroon, 1994). The eight bar configurations are: infragravity scaled surf zone, infragravity scaled 2-D bar, non-rhythmic 3-D bar, offshore rhythmic bar, attached rhythmic bar, non-rhythmic attached bar, incident scaled bar and reflective beach with no bars (Lippmann and Holman, 1990). These eight distinct bars types are defined by four independent morphology and hydrodynamic criteria: 1) existence or absence of a bar; 2) dominant bar scaling (incident vs. infragravity); 3) longshore variability (linear, rhythmic or non-rhythmic); and 4) trough (continuous or discontinuous). The authors note that these criteria are related to processes thought to be important in controlling nearshore morphology, particularly bar scaling and longshore variability (Lippmann and Holman, 1990). This classification provides a first-order approximation of offshore (accretional) and onshore (erosional) bar migration sequences that can be applied to different environments (Lippmann and Holman, 1990). While Wright and Short (1984) were the first to utilize a holistic approach, Lippman and Holman (1990) were the first to apply remotely sensed techniques on the nearshore environment. This has made Lippman and Holman (1990) the baseline for contemporary bar classification and identification studies (c.f., Gallangher et al., 1998; Masselink and Short, 1993; Ranasinghe et al., 2004).

1.3 High-energy events and coastal system changes

Coastal system changes occur at a wide range of spatial and temporal scales (Houser et al., 2008; List et al., 2006; Morton et al., 1994). High-energy events can be generated by tropical or extratropical systems, and winter storms. It is important to clarify that, in our current study, high-energy wave events are weather systems that cause elevated wave heights (e.g., tropical storms,

mid-latitude cyclones, or winter storms). In response to single storm events, the expected beach response is a transition from a berm or fair-weather profile to a steep storm profile (Davidson-Arnott, 2010; Komar, 1998; List et al., 2006). Studies have documented significant longshore variations in shoreline change in response to a single high-energy event (i.e., a storm) (Houser et al., 2008; List and Farris, 2009; Sallenger et al., 2003; Stockdon et al., 2002). It has been observed that there is a non-uniform shoreline response to storms, in which portions of the coast have significant erosion alternating with sections of coast that were almost entirely unaffected (Aleman et al., 2017; Houser and Hamilton, 2009; List and Farris, 2009; List et al., 2006; Stockdon et al., 2002).

Early studies attributed the variability of beach erosion and recovery rates after high-energy wave events to longshore differences in crescentic bar morphology or small gaps in parallel bars (Sonu, 1973; Zeigler et al., 1959). Some studies focused on the effects of tropical cyclones on the coastal system (Houser and Hamilton, 2009; List et al., 2006). These studies looked at the effects of a single storm on the system as well as the cumulative effects of multiple storms (Aleman et al., 2017; Houser and Greenwood, 2007; Houser et al., 2008; Houser and Hamilton, 2009). Other studies considered the effects of winter storms on the beach, dune, and nearshore bar systems (Houser and Greenwood, 2001). These studies examine the effects of multiple winter storms in the coastal spanning decades (Aleman et al., 2017; Houser and Greenwood, 2001). Beach recovery cycles may be connected to the migration of what was then referred to as 'rhythmic shoals' (Sonu, 1973). As bars continue to migrate onshore, they may eventually weld to the shore resulting in beach accretion (Aagaard et al., 2005; Aleman et al., 2017; Houser and Hamilton, 2009; Davidson-Arnott, 2010). Bar welding can occur in areas where bars continue to exist (multiple bar systems) in the nearshore and does not only occur at sites where bars were only generated during a storm event (Aagaard et al., 2005). Nearshore bars have a controlling influence on the beach-dune response to storms (List et al., 2006; Ziegler et

al., 1959). Portions of the coastal system that exhibit high erosion rates had no bars in the nearshore prior to the storm, allowing more wave energy to penetrate closer to the shore (Aleman et al., 2017; List et al., 2006; van de Lageweg et al., 2013; Ziegler et al., 1959). In contrast, parts of the coastal system with one or more nearshore bars present have significantly lower erosion rates since the bars dissipate offshore wave energy (List et al., 2006; Ziegler et al., 1959).

Here we investigate how bar morphology influences beach-dune response to high-energy wave events by analyzing pre- and post-event multispectral imagery and assessing changes to the beach, dune, and bar systems. High-energy wave events can be produced from tropical cyclones or winter storms. Proximity of the bar to the wet/dry line can be used to examine beach-dune response. Response, in this case, is defined as the post-event rebuilding process where there is an onshore return of sediment to the subaerial beach during non-storm conditions (Jensen et al., 2009; Morton and Sallenger, 2003; Phillips et al., 2017).

1.4 Study Area

Three coastal systems are observed to assess the influences of nearshore bars on beach-dune responses to high-energy wave event conditions (Figure 4.2). The study site characteristics and dynamics are summarized in Table 4.1 using data from existing infrastructure (meteorological stations and buoys). These meteorological stations and buoys record wave data every 20-minutes (height, period, and direction) and wind data (speed and direction) every 8-minutes at the buoys and 2-minutes for the land-based stations. Wind data are obtained for all study sites to characterize the climatology of the location. The selected sites are:

A) *Duck, North Carolina, USA* (intermediate beach state): This site has a rhythmic single bar system that varies from a longshore to a crescentic bar depending on wave

conditions. The study area at Duck covers 1 km of the coast, including a well-developed and vegetated dune system. This coast faces east to the Atlantic Ocean and has a bimodal wind pattern receiving the strongest winds from the SSW during the hurricane season (June-November) and from the NNE during the winter season (December-March). April to May winds are from the west. Year-round wind speed averages 5 m/s based on three years of data (2014-2016) (Figure 4.2A; A').

B) *Cassino Beach, Rio Grande do Sul, BRA* (dissipative beach state): This Brazilian beach is characterized by coastal dynamics similar to those found on the west coast of the United States with 1-2 bars typically present. This beach also has a well-developed dune system. Cassino Beach and Bay St. Louis are both dissipative beaches, but their wave climate conditions are substantially different with Cassino experiencing larger waves (see Table 4.1). This coast is oriented SSE, facing the South Atlantic Ocean, with a multidirectional wind pattern that receives the fastest velocity winds during the winter season (June-September). There is a peak of wind coming from the southwest during the winter, mainly during the month of June, when this area experiences a high incidence of severe storms (Melo et al., 2016). Lower velocity wind speeds are observed between October and May. Year-round wind speed averages 8 m/s based on three years of data (2015-2017) (Figure 4.2B; B').

C) *Bay St. Louis, Mississippi, USA* (dissipative beach state): A well-developed bar system is located at Bay St. Louis, Mississippi. This study area covers 0.87 km of the coast. The shoreline is oriented SSE facing the Gulf of Mexico. The wind pattern is

bimodal, which is most likely related to the sea breeze dynamics from the region (at night the wind comes from the land (N-NE), during the day from the ocean (S-SE). Year-round wind speed averages 7 m/s based on three years of data (2015-2017) (Figure 4.2C; C'). During this time. the strongest winds were recorded from SSE and were linked to the hurricane season between June and November.

Table 4.1. Study site characteristics. Reflective beaches were not considered for this study since they are often considered barless (Hesp, 2012; Short and Hesp, 1982; Wright and Short, 1982).

Location	Tidal regime	Wave height range	Wave period range	Meteorological station / buoy	Meteorological station / buoy distance from site
Duck, NC	0.7-1.5 m	0.5-2.0 m	8-10 s	44056[†] / ORIN7[∞]	11.03 km / 37.52 km
Cassino Beach, RS	0.5-1.0 m	1.0-1.5 m	6-12 s	31053[*] / n/a	88.03 km / n/a
Bay St. Louis, MS	0.1-0.7 m	0.3-1.0 m	0.5-3 s	WYCM6[‡] / 42067[**]	0.28 km / 71.86 km

[†]Buoy operated and maintained by U.S. Army Corps of Engineers and downloaded from the NOAA National Buoy Data Center (NDBC) website.
[∞]Meteorological station owned and maintained by NOAA's National Ocean Service, data downloaded from the NOAA NDBC website.
[*]Buoy owned and maintained by the Brazilian Navy Hydrographic Center, data provided by Dr. Lauro Calliari, from the Federal University of Rio Grande, Brazil.
[‡]Meteorological station owned and maintained by NOAA's National Ocean Service, data downloaded from the NOAA NDBC website.
[**]Buoy operated and maintained by the University of Southern Mississippi, data downloaded from the NOAA National Buoy Data (NDBC) website.

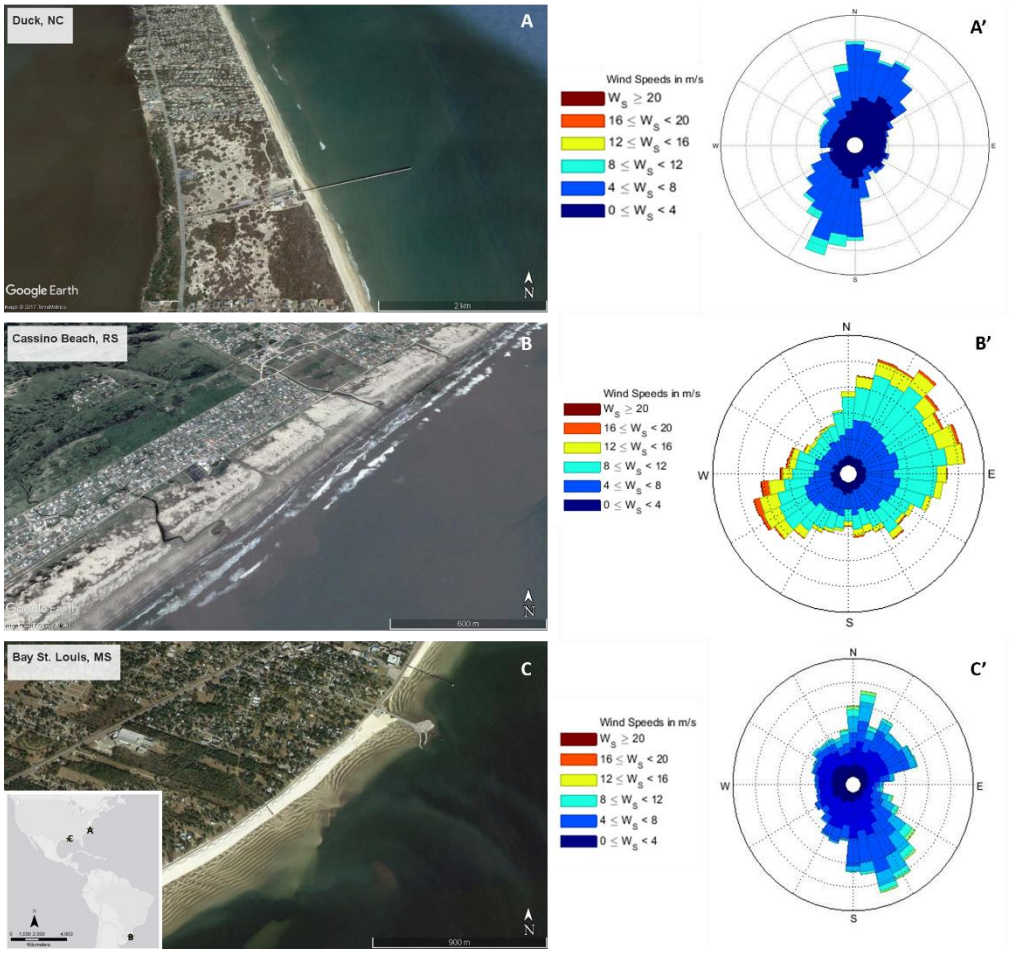

Figure 4.2. The three study sites: A) Duck, NC, A') wind data obtained from NDBC buoy ORIN7 located 35.47 km SSE to show conditions at the Duck site; B) Cassino Beach, RS, B') wind data obtained from Brazilian Navy Hydrographic Center buoy 31053 located 88.03 km directly east of the Cassino Beach site; C) Bay St. Louis, MS, C') wind data obtained from NDBC meteorological station WYCM6 located 0.28 km north of the Bay St. Louis study site. The inset map in the lower left of A, B, and C shows the geographic locations of the three sites.

2 Methodology

2.1 High-Energy Wave Event Identification

To understand the system-wide response to high energy wave events, we used wave data to determine 'non-event' and 'event' (i.e., tropical cyclones or winter storms) conditions at each study site. As observed in previous studies (Aleman et al., 2017; Houser and Greenwood,

2007; Houser et al., 2008; Houser and Hamilton, 2009), we anticipated geomorphic changes to the beach-dune-bar systems after an event or events. Wave data were acquired from the closest buoy to each study site (Table 4.1). We obtained approximately one calendar year (Duck, NC: January to September 2014; Cassino Beach, RS: January to December 2017; Bay St. Louis, MS: January to September 2017) of buoy data (Table 4.2) that aligned with the multispectral image acquisition year. These data were quality controlled to remove all empty or erroneous points. Empty or erroneous points occur when the sensors do not record data for a particular time or when the sensor records values of "99" or "999" instead of a realistic measurement. The wave climate data for the site at Duck, NC and Bay St. Louis, MS were obtained from the National Data Buoy Center (NDBC) website (www.ndbc.noaa.gov), while the data for Cassino Beach were provided by Dr. Lauro Calliari from the Federal University of Rio Grande, Brazil.

High energy wave events were identified using a threshold based on *significant wave height* (H_s), which is the mean wave height of the highest one-third of waves observed during a particular time period. The *significant wave height* at each site ($H_{s\text{-}site}$) was calculated using approximately one calendar year of wave data (Table 4.2) from the buoy. This study defined high energy wave events as periods of at least 6 hours when wave heights consistently exceed $H_{s\text{-}site}$ (c.f., Dolan and Davis, 1992; 1994; Hill et al., 2004; Rangel-Buitrago and Anfuso, 2011; Splinter et al., 2014). The event was defined as the duration from the first time (start) the buoy registered wave heights exceeding the calculated $H_{s\text{-}site}$ to the last successive time before $H_{s\text{-}site}$ fell below the threshold (end) (Castelle et al., 2015; 2017; Splinter et al., 2014).

After the events that exceeded the threshold were identified, the buoy data were corroborated with data from the National Weather Service (NWS) or the Instituto Nacional

de Meteorologia where we obtained the characteristics of the event-associated weather systems. Some weather systems may produce multiple high energy wave events, that is, multiple periods of time where $H_{s\text{-}site}$ was exceeded for longer than 6 hours. The NWS and Instituto de Nacional Meteorologia data were consulted only to obtain weather system characteristics; the high energy events were solely identified using the wave height data obtained from the buoys. The selected events and the associated wave characteristics are presented in Table 4.2 and discussed below.

Table 4.2 Selected weather systems and corresponding wave characteristics during the high-energy wave events, where H is mean wave height, $H_{s\text{-}event}$ is the significant wave height during the event, and H_{max} and H_{min} are maximum and minimum wave heights, respectively, recorded during the events. High energy events produced by the same weather system were merged to create this table.

Location	**Weather System Characteristics**		**Weather System Wave Characteristics**			
	Dates	**Event duration (hours)**	H **(m)**	$H_{s\text{-}event}$ **(m)**	H_{max} **(m)**	H_{min} **(m)**
Duck, NC	01/22-23/2014	29	2.70	3.76	3.82	1.91
	01/27-29/2014	40	2.37	2.60	2.77	1.94
	02/04-05/2014	9	1.99	2.06	2.07	1.93
	02/12-22/2014	28	2.18	2.80	3.05	1.61
Cassino Beach, RS	05/18-22/2017	101	4.61	5.46	6.70	3.28
Bay St. Louis, MS	06/20-23/2017	27	2.60	3.11	3.39	1.37

The 2014 Winter Storm season was an active one for the Duck, NC; four significant systems affected this region between the selected dates. The first winter storm was a fast-

moving disruptive blizzard that moved through the Northeast generating significant surge along the eastern seaboard (NWS, 2014). The system was at its peak on January 22nd with the lowest atmospheric pressure of 962 mb, but wave heights in the area did not exceed the $H_{s\text{-}site}$ threshold of 1.88 m Duck, NC until January 23rd. The second storm was a low-pressure system that formed near the western Gulf of Mexico on January 27th and eventually moved eastward (NWS, 2014). Coastal regions along the southeast including the Outer Banks received significant amounts of snow and ice, which led to closings of roads and bridges across the region. On February 4th Duck, NC experienced on and off wave heights higher that the $H_{s\text{-}site}$ threshold of 1.88 m associated to a cold front of the northeast coast that affected the area until February 6. Only one high-energy wave was identified for this weather system as the threshold was exceeded for 9 hours on 2/04/2014 (between 4:00AM and 1:00PM). The $H_{s\text{-}site}$ was exceeded twice more during the weather system but not for more than 6 hours (on 02/04/2014 for an hour at 7:00PM and on 02/06/2014 for 2 hours between 12:00-1:00PM). Lastly, a significant winter storm affected the region between February 12 to the 24th, which brought a lot of ice to the Carolinas. North Carolina snow totals ranged between 6-12 inches in some areas, along with accumulating ice (NWS, 2014). This weather system produced two periods where significant wave heights exceeded the $H_{s\text{-}site}$ threshold and lasted for more than 6 hours. There was a period of 7 hours of sustained $H_{s\text{-}site} > 1.88$ m on 02/12/2014 between 9:00AM and 3:00PM, and a period of 21 hours on 02/13/2014 between 2:00AM and 10:00PM. A wave height reading that exceeded the $H_{s\text{-}site}$ threshold was recorded on 02/22/2014 but it was not included in the analysis because it was only for 1 hour (at 4:00AM).

At Cassino Beach, we considered a storm that occurred between May 17th thru the 29rd that produced wave heights exceeding the $H_{s\text{-}site}$ threshold for this site for a continuous 101 hours. According to local meteorological stations, more than 300 mm of rain fell in the region in 24 hours on May 28th (Instituto Nacional de Meteorologia, 2017). In Rio Grande do Sul, 48 municipalities reported damages due to large hail and fast winds (Instituto Nacional de Meteorologia, 2017). There were other instances, in the available dataset, where the $H_{s\text{-}site}$ was exceeded, but the temporal duration did not exceed 6 hours, therefore they were not classified as high energy wave events.

Lastly, at Bay St. Louis, we analyzed Tropical Storm Cindy that affected the study area June 20-23, 2017. According to the National Hurricane Center (https://www.ncdc.noaa.gov/sotc/tropical-cyclones/201706), Tropical Storm Cindy formed from an area of low pressure near the Yucatán Peninsula. It moved northward strengthening to tropical storm when it reached the Gulf of Mexico on June 20, 2017 south of Louisiana. At its maximum strength, Tropical Storm Cindy had winds of 27 m/s. Tropical Storm Cindy weakened before making landfall near the Louisiana/Texas border on June 22, 2017, approximately 445 km west of Bay St. Louis.

Once the high-energy wave events were identified, the corresponding pre- and post-event satellite images (WorldView series, Digital Globe) were acquired for each study site (Table 4.3). We targeted imagery that could capture the site conditions closest to the start (pre-event) and end (post-event) of the weather system, and that has relatively clear water and that was collected during periods of low wave energy; the last two points are required for successful execution of the image classification methods (see Section 2.2 and Chapter 3). The imagery was used to obtain nearshore bar system and beach-dune parameters.

Specifically, the bar characteristics that we measured were bar length, width, count, distance from the bar edge to the wet/dry line, and morphology following the Lippmann and Holman (1990) classification. The beach-dune parameters we measured were beach and dune width. These parameters were calculated to compare conditions at each location before and after the storm event.

Table 4.3 Multispectral imagery metadata

Location	Image Acquisition Date		Source	Resolution	
	Pre-event(s)	Post-event(s)		Spectral	Spatial
Duck, NC	01/15/2014	03/09/2014	World-View 2	4 bands	50 cm
Cassino Beach, RS	05/12/2017	07/16/2017	World-View 3	4 bands	30 cm
Bay St. Louis, MS	06/13/2017	06/27/2017	World-View 2	4 bands	50 cm

2.2 Rule-Based Image Classification

To identify the beach-dune and nearshore bar parameters, a rule-based image classification was completed at each site. Imagery with increased spatial resolution favors the object-based classification methods (OBIA) over per-pixel classification analyses because it allows the analyst to look at an object composed of more than one pixel (Blaschke, 2010; Heumann, 2011). In OBIA, an object is composed of a group of pixels and is first segmented into representative shapes and sizes. The resulting objects represent meaningful features in the image that allow the analyst to classify objects based on texture, context, and geometry (Blaschke, 2010; Blaschke and Strobl, 2001). Further, in a rule-base classification, similar objects are grouped into classes (Bouziani et al., 2010; Tarabalka and Tilton, 2012). Each

generated class contains one or more decision rules based on the users' knowledge of the feature being classified. These rules may contain one or more attributes, such as spectral, spatial, or texture with user-defined ranges of values.

The classification process in this study was completed using the Feature Extraction Module (ENVI Fx) for ENVI 5.5.1 following the steps described in Chapter 3. After the attributes for each feature (dune, beach, and nearshore bars) were computed, the features were extracted using a similar rule-based classification method, but applied exclusively to the dunes and beach (Delgado-Fernandez et al., 2009; Hugenholtz et al., 2012; Ryu and Sherman, 2014). The rules applied to identify the features were based on the spectral values of the features for each image (Table 4.4).

Table 4.4 Spectral values used for rule-based classification method. The green band was used to segment the images and acquire pixel values

Location	Date	Feature	Pixel Values
Duck, NC	Pre-events	Dune	68.100-70.00
		Beach	205.00-214.00
		Bars	175.61-247.50
	Post-events	Dune	68.15-70.16
		Beach	204.36-215.00
		Bars	No bar identified
Cassino Beach, RS	Pre-event	Dune	73.39-90.60
		Beach	100.60-115.79
		Bars	117.37-155.85
	Post-event	Dune	74.40-92.00
		Beach	109.69-116.30
		Bars	No bar identified
Bay St. Louis, MS	Pre-event	Dune	68.18-70.19
		Beach	205.26-215.01
		Bars	121.93-164.27
	Post-event	Dune	68.10-70.01
		Beach	205.01-216.01
		Bars	120.66-164.26

After the imagery is processed, the results showing the post-event changes to the beach-dune system were compared to the nearshore bar morphodynamics to determine the coastal system response. Proximity of the bar to the wet/dry line was the parameter evaluated to identify specific characteristics of the nearshore in relation to the response stages of the dune and beach at each site.

3 Results

3.1 Duck, NC

This study site is located within the US Army Corps of Engineers (USACE) Field Research Facility and there are little to no anthropogenic influences affecting this coastal area. The pre-events image on 01/15/2014 presented a discontinuous longshore single bar that extended along the 1 km study area. The bars had an average width of 3.6 m and were located at an average distance of 133.4 m from the wet/dry line. The beach had an area of 0.02 km^2 and foredune system 1 was located at an average distance of 30.3 m from the wet/dry line. Two hotspots of erosion (shown in Figure 4.3A as red arrows) are aligned with gaps on the discontinuous bar. The post-events image analyzed was from 03/09/2014, 53 days after the pre-events imagery. There was no other image available at an earlier date that fulfilled the criteria for the study. Four winter storms affected the region between the acquisition of the two images (January 22-23, January 27-29, February 4-5, February 12-24; Table 4.2). The analysis is not capturing the immediate response of the coastal system to the weather systems and therefore it is possible that our results are influenced by the early stages of recovery since the post-events image was captured 16 days following the last high energy wave event.

Comparing the two images, the beach area remained at 0.02 km^2. Foredune system #1 showed reduction of 2.2 m (0.3%). The post-events duneline presented two new hotspots of erosion (Figure 4.3B with the solid red arrows), which aligned with the gaps identified in the discontinuous bar (Figure 4.3A, yellow arrows). A second receding gap to the left of the pier can be identified following the storms (in Figure 4.3B) 2 m to the west of the one previously identified (Figure 4.3A). The beach width varied approximately 16.4 m between the pre- and post-events conditions, based on measurements obtained from 10 transects along the study site that extended from the duneline to the wet/dry line.

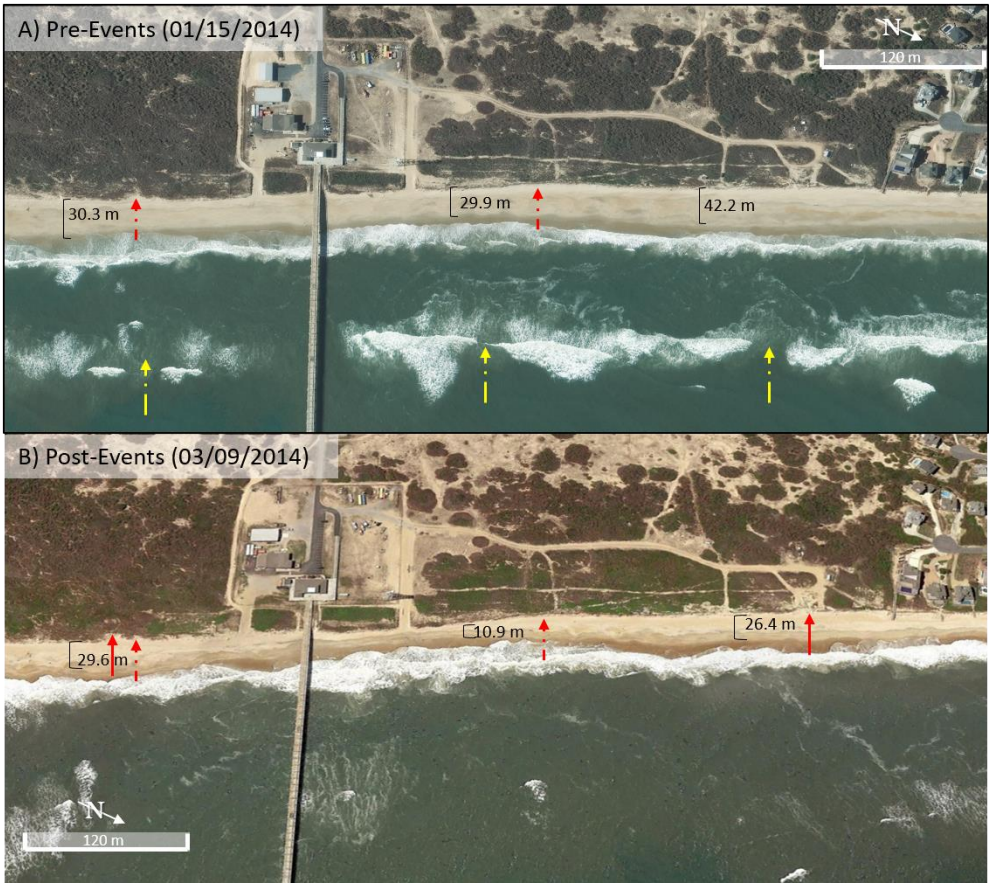

Figure 4.3 Results of the pre- (A) and post-events (B) imagery analysis for Duck, NC. (A) The yellow arrows show the gaps in the discontinuous nearshore bar. The dashed red arrows show the areas of dune erosion. (B) No bar was identified post-events; dashed red arrows show the same location as the previous image, solid red arrows show new 'hotspot' areas of erosion following the high-energy wave events. Image (B) is at a slight angle due to an imagery offset.

3.2 Cassino Beach, RS

Cassino Beach has a well-developed dune system. The 1 km study area is demarcated by two mud banks. This area is mainly affected by storms associated with winter weather. This site has western, center, and eastern portions, which are delineated by beach access points. A single longshore bar system was identified at this site in the pre-event image on May 12, 2017. On this date, the bar measured 455.8 m in length, with an average width of 25.6 m. The beach area was 0.07 km^2, with the width (or distance from the dune to the wet/dry line) varying from 111.9 m on the west end (foredune #1), 77.9 m in the center (foredune #2) and 79.9 m on the eastern portion (foredune 3) of the beach (Figure 4.3A). The dunes are well-developed with three clusters that are separated by the beach access points. Foredune #1 on the west end extends 488.8 m and has an area of 0.13 km^2. Foredune #2 in the center portion of the study area has a length of 446.1 m and an area of 0.12 km^2. Lastly, the easternmost portion of the foredune has a length of 335.8 m and an area of 0.08 km^2.

The post-event image was obtained on 07/16/17, 57 days after maximum wave height. There are no wave records available for the buoy between 6 June and 9 September 2017. Instead, the available wave record shows another event between May 28-30 that generated wave heights higher than the $H_{s\text{-}site}$ threshold, but the wave heights that exceed the threshold are not sustained for a period of more than 6 hours and therefore was not classified as a high-energy wave event. No nearshore bar was identified for the study site in the post-event image. The beach width and dune systems remained relatively stable. The beach area decreased to 0.06 km^2 (14.3% difference), with the beach width in front of the western (foredune #1) and eastern (foredune #3) portion eroding to average widths of 85.3 m and 65.4 m, respectively. The center portion of the beach showed a widening of 82.7 m. The

length of the foredunes varied between 0.1% (foredune #1) and 0.2% (foredune #2) (Figure 4.3B, Table 4.4), with the central foredune expanding 12.8 m (2.9%). The foredune areas were also largely maintained; the maximum change was at the central foredune (+8.3%).

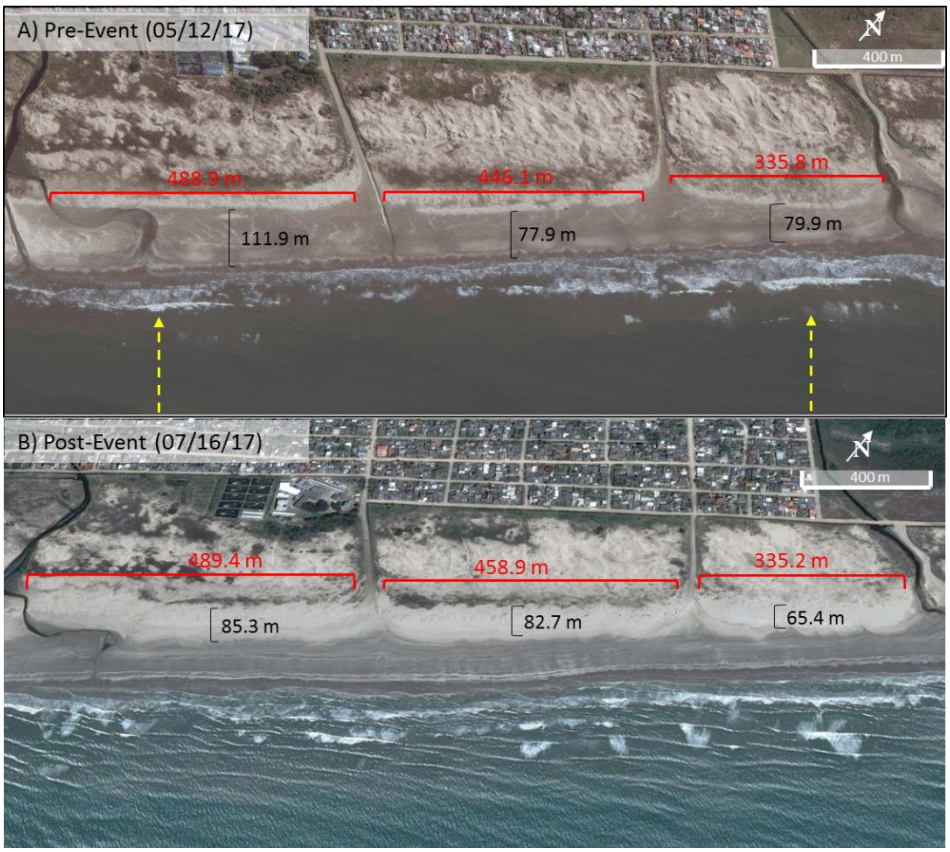

Figure 4.4 Results of the pre- (A) and post-events (B) imagery analysis for Cassino Beach, BRA. (A) Pre-event conditions, (B) post-event conditions, no bar was identified in the post-event image. Hatched yellow arrows show the location of the identified bar.

3.3 Bay St. Louis, MS

The study area at Bay St. Louis underwent a flood and a coastal storm damage reduction project in 2015. This project included the construction of a concrete seawall structure dividing the beach from the main road, the completion of a small beach nourishment project, and the emplacement of 30 dune-like structures. The impetus for this project was to revitalize the area 10 years after Hurricane Katrina.

A well-developed multiple bar system was identified at Bay St. Louis before Tropical Storm Cindy on 09/13/17. A combination of longshore (located in the outer bars, those located further from the shoreline) and crescentic bars (located in the inner bars, those located closer to the shoreline) were identified. The bar system was better developed on the western portion of the site with eight longshore bars that had an average length of 0.8 m and an average width of 0.5 m. The eastern portion of the bar contained six bars that extended the length of the study site. The crescentic bars were identified close to the shoreline (15.0 m) and had an approximate width of 7.0 m. The beach had an area of 0.06 km^2, but the width varied alongshore. The western portion of the beach, where most of the bars where identified, was the narrowest part (59.4 m). The center and eastern portion of the beach were the widest locations with measurements of 84.8 m and 88.3 m, respectively (Figure 4.5A). Thirty dune-like structures, which are considered one dune system, were identified with a pre-event average length of 32.9 m.

The post-event image was acquired on 9/27/17, 6 days after peak wave height. The bar system remained unchanged with 8 bars identified on the western portion of the study site, while four bars longshore bars were identified in the eastern portion of the study area. Crescentic bars were also found in the inner portion of the nearshore bar system, similar to the pre-event conditions. Bar width varied only a few centimeters (see Table 4.4). The beach area changed 16.7% with the area increasing to 0.07 km^2. As shown in Figure 4.5B, distance of the dune to the wet/dry line varied slightly with the eastern corner (foredune #1) accreting 0.3 m (0.5%), the center portion (foredune #2) accreting 0.4 m (0.5%), and the western corner (foredune #3) of the study site eroding 13.0 m (-16.2%). The dune-like features were

all accounted for in the post-event image and remained unchanged, from a length and area perspective.

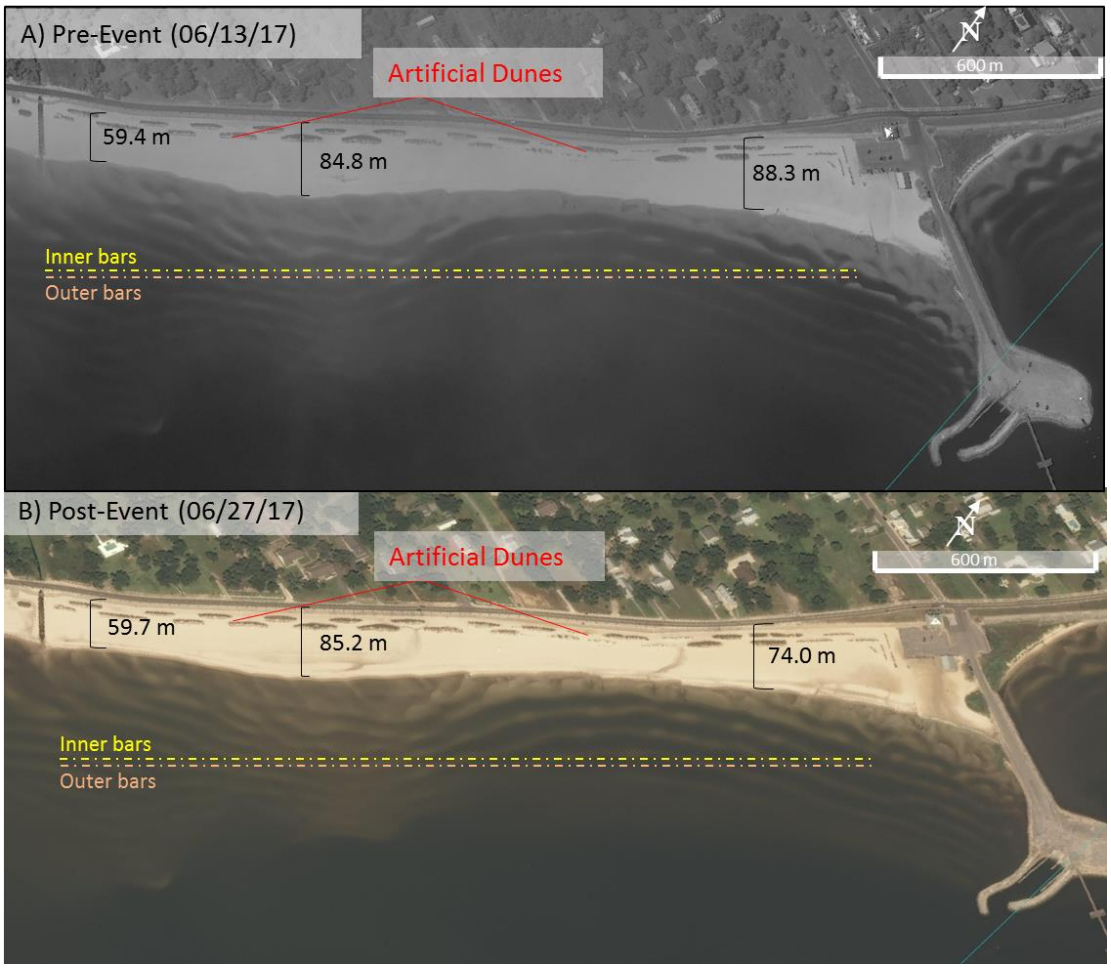

Figure 4.5 Results of the pre- (A) and post-event (B) imagery analysis for Bay St. Louis, MS. (A) Pre-event conditions, while (B) shows post-event conditions. This site has a multiple bar system comprising longshore bars in the outer portion (farthest from the shore; offshore of orange hatched line) and crescentic bars in the inner portion (closer to the shore; onshore of yellow hatched line).

4 Discussion

Nearshore bars are intrinsically linked to the beach-dune system. Not only does sand cycle from the nearshore to the beach and from the beach to the dune system, but also it protects the beach-dune system from high energy events such as storms. This study looked at three

distinct locations to assess how nearshore bar morphology influences beach-dune characteristics during high-energy wave events and how these relationships vary geographically. Results showed that in all instances the portions of the beach located directly onshore to longshore bars (Duck, NC and Cassino Beach, RS) or crescentic bars (Bays St. Louis, MS inner bar system) were protected from the high-energy wave events (Table 4.5). Unfortunately, a true comparison between sites was not possible since some study areas experienced a different number of high-energy wave events than others. Duck, NC experienced four weather systems, with 5 high-energy wave events, Cassino Beach, RS experienced one event, but a portion of the record is missing so we cannot rule-out the possibility of other high-energy wave events affecting the area between the pre- and post-event imagery, while Bay St. Louis, MS also experienced one high-energy wave event. Nevertheless, it is still possible to examine the response of the coastal systems to these events and conceptualize how nearshore bars can or cannot protect these systems from potential erosion caused by high-energy wave events.

Using the rule-based classification approach from Chapter 3, we identified key features in the coastal system such as the bar morphology and characteristics, duneline location and extent, and beach width (or distance from the wet/dry line). These results were analyzed to understand how the nearshore bars influence dune-beach responses after experiencing one or more high-energy wave events. Results also demonstrated that the bar morphology influences how the dune and beach responds to high-energy wave events. Figure 4.6 presents a modification of Masselink and Hughes (2003) to illustrate the observed relationship between bar morphology and the dune and beach system.

Table 4.5 Characteristics of bars at the three study sites extracted from the rule-based classification.

BARS	Duck NC Pre-Events	Duck NC Post-Events	*Percent Change*	BSL, MS Pre-Event	BSL, MS Post-Event	*Percent Change*	Cassino Beach, RS Pre-Event	Cassino Beach, RS Post-Event	*Percent Change*
Bar System 1									
Width (m)	3.6	n/a		0.5	0.4	*-20.0%*	25.6	n/a	
Distance from wet/dry line (m)	133.4	n/a		7.0	6.0	*-14.3%*	33.7	n/a	
Length (m)	103.5	n/a		0.8	0.9	*12.5%*	455.8	n/a	
Bar System 2	n/a						n/a		
Width (m)				7.0	7.5	*7.1%*			
Distance from wet/dry line (m)				15.0	14.7	*-2.0%*			
Length (m)				1.0	0.9	*-10.0%*			
BEACH									
Area (km^2)	0.02	0.02	*0%*	0.06	0.07	*16.7%*	0.07	0.06	*-14.3%*
DUNES									
Foredune System 1									
Average length (m)	355.7	355.7	*0.0%*	32.9	32.9	*0.0%*	488.9	489.4	*0.1%*
Area (km^2)	872.3	870.1	*-0.3%*	252.0	250.0	*-0.8%*	0.13	0.13	*0.0%*
Distance to wet/dry line (m)	30.3	29.6	*-2.3%*	59.4	59.7	*0.5%*	111.9	85.3	*-23.8%*
Foredune System 2									
Average length (m)	n/a	n/a	n/a	n/a	n/a	n/a	446.1	458.9	*2.9%*
Area (km^2)	n/a	n/a	n/a	n/a	n/a	n/a	0.12	0.13	*8.3%*
Distance to wet/dry line (m)	29.9	10.9	*-63.5%*	84.8	85.2	*0.5%*	77.9	82.7	*6.2%*
Foredune System 3									
Average length (m)	n/a	n/a	n/a	n/a	n/a	n/a	335.8	335.2	*-0.2%*
Area (km^2)	n/a	n/a	n/a	n/a	n/a	n/a	0.08	0.07	*-12.5%*
Distance to wet/dry line (m)	42.2	26.4	*-37.4%*	88.3	74.0	*-16.2%*	79.9	65.4	*-18.1%*

The diagram shows the spatial relationship between dune erosion hotspots areas where there is no bar or a weak spot in the bar morphology (Figure 4.6). Continuous

longshore bars (Figure 4.6A) provide the most protection by attenuating waves, since they tend to migrate offshore during storm conditions (Houser and Greenwood, 2007; Houser and Hamilton, 2009). Wave energy is attenuated as the waves *shoal* (or 'feel bottom') when approaching the shallower depths of the nearshore bars.

This dynamic was best observed at Cassino Beach, RS where in the pre-event image there was a single continuous longshore bar system that protected the beach and dune system. The beach was widest and presented the least amount of change in the locations directly onshore of the continuous longshore bar system (Table 4.5). From an area perspective, the westernmost foredune (foredune system 1) remained unchanged, the center foredune area (foredune system 2) accreted 8.3% and the easternmost foredune area (foredune system 3) eroded 12.5%. The erosion observed at both the easternmost and westernmost foredune distance from the wet/dry line (23.8% and 18.1%, respectively) could have been linked to the creek that flows to the ocean in those sections moving closer to the dune line for the post-event imagery (Figure 4.4). These observations of foredune distance from the wet/dry line erosion at the easternmost and westernmost foredune (foredune systems 1 and 3) might have also been influenced by the tidal stages at which the pre- and post-event images were taken. The pre-event image was taken during low tide conditions while the post-event image was taken during high tide conditions. The difference in tidal range was 0.20 m (Table 4.5). This difference contributes to the observation of narrower beach during the post-event image.

This pattern was also observed at Bay St. Louis, MS (Figure 4.5) where a combination of the outer bar system of continuous longshore bars and inner bar system of crescentic bars protected the beach and dunes at this location. The beach area accreted

approximately 16.7% (Table 4.5). The average length of the artificial dunes remained largely unchanged (<3% change) between the pre- and post-event measurements. The distance from the wet/dry line reveals that there was some accretion on the easternmost and center portion of the site, while the westernmost portion of the site experienced the most erosion area as shown by the distance from the wet/dry line of the foredune system 3 (16.2% change). Tidal stage did not play a role in influencing the results at this location, since the pre- and post-event images were taken at high tide and presented the same tidal elevation (Table 4.6).

Discontinuous longshore bars (Figure 4.6B), on the other hand, still offer some protection to the dune-beach system by attenuating waves, but also cause erosion hotspots in the dune sections onshore to the gaps between the bars. This was observed at Duck, NC where two segments of the duneline showed that the distance from the wet/dry line increased 2.3% and 37.4% after the high-energy wave event. These variations at this location might have also been influenced at this location by the tidal stages and elevation differences between the pre- and post-events images. The pre-events image (01/15/2014) was taken at low tide with a MLLW elevation of 0.00 m, while the post-events image (03/09/2014) was taken at high tide with a MLLW elevation of 0.76 m (Table 4.6). We have to also consider that, based on the available buoy data, this site experienced 5 high-energy wave events between the pre- and post-event imagery, which may contribute to the higher erosion percentages in the beach and dune area.

Although not observed in isolation at any of the sites, we posit crescentic bars would have a similar effect on the dune-beach system as discontinuous bars (Figure 4.6C, D). Beaches where crescentic bars are present, such as Bay St. Louis, will have varying widths across the beach (Bruneau et al., 2009; Castelle et al., 2016). The locations where the crest of

the bar (convex portion of the crescentic bar) is onshore to the beach will be better protected, because the waves will be attenuated, while the horns of the bar (concave portion of the crescentic bar) are a weak point allowing waves to break closer to the shoreline creating beach cusps and generating rip currents that move sediment and cause hotspots of erosion at the dune (Bruneau et al., 2009; Castelle et al., 2016; Castelle and Coco, 2012; Dalrymple et al., 2011;Figure 4.6C, D).

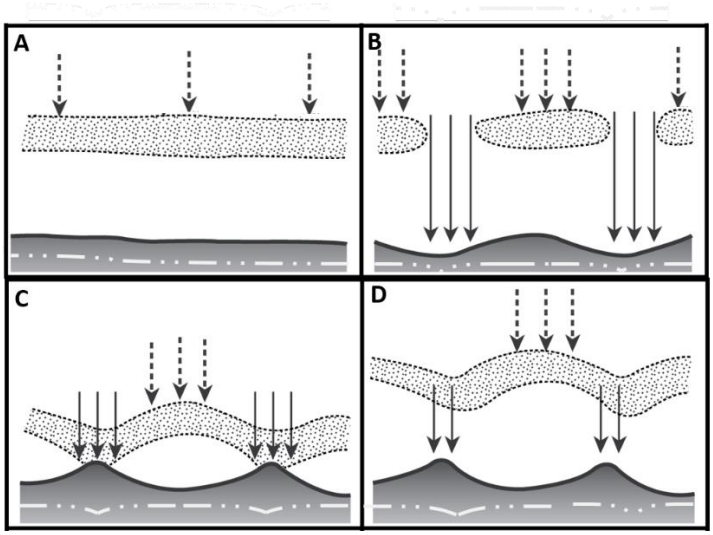

Figure 4.6 Panels A, B, C, and D show how bars attenuate waves and the impact to the beach/dune system. Hatched arrows show the areas where waves are expected to be attenuated, solid arrows show the weak points where the waves reach the beach. The white hatched lines depict the position of the duneline in each scenario. A) Longshore bar; B) Discontinuous longshore bar; C) Shore-attached crescentic bar; D) Crescentic bar.

The results also reveal high percentages of change for the beach area and average distance from the wet/dry line to the dune variables particularly at Duck, NC and Cassino Beach, RS (Table 4.4), which may be due to the amount of high-energy wave events that affected the area between the pre- and post-event imagery analysis as the system may have not time to recover from one event before it is affected by another. In the cases where beach area erosion exceeds 12%, this activity can be attributed to the position of the wet/dry line in

the particular image analyzed. While there are many concerns about using the wet/dry line as proxy since this line fluctuates daily (in some areas twice a day) due to variations in water level, tidal range, and wind and wave conditions (Plant and Holman, 1997; Thieler and Danforth, 1994), which can be impacted by image acquisition time, it is still the most commonly used proxy for shoreline position (Moore, 2000; Shoshany and Degani, 1992). Due to the variability of the location of the wet/dry line, different researchers use different identification features to define the line.

Table 4.6 Image acquisition time and tidal stage, time, and height at each study site. All tides are referenced to mean low low water (MLLW) levels.

Location	Date	Image Acquisition Time	Tidal Stage / Time/ Height (m)
Duck, NC[†]	01/15/2014 03/09/2014	4:12PM 4:06PM	Low / 1:17 PM / 0.00 m High / 2:59 PM / 0.76 m ***Difference: 0.76 m***
Cassino Beach, RS[*]	05/12/2017 07/16/2017	11:30AM 11:10AM	Low / 10:19AM / 0.10 m High / 7:26 AM / 0.30 m ***Difference: 0.20m***
Bay St Louis, MS[‡]	06/13/2017 06/27/2017	3:25PM 3:05PM	High / 2:18PM / 0.61 m High / 2:08PM / 0.61 m ***Difference: 0.00 m***

[†]Data obtained from station 8651370 located in the Pier at the USACE Coastal Field Research Facility in Duck, NC.
[*]Data obtained from the tidal gauge at Porto do Rio Grande, Brazil.
[‡]Data obtained from the Bay Waveland Yacht Club station (ID: 8747437) located in Bay St. Louis, MS.

Some examples include maximum run-up during a rising tide that affects part of the beach that is still wet during the falling tide (Overton et al., 1999), distinct edge in image based on brightness between the wet and dry beach areas (the technique employed in this study; Hoeke et al., 2001), and land/water boundary shown by a variation in color or gray tone (Douglas et al., 1999). Despite the variability of the wet/dry line, techniques like the ones described above allow for the use of the wet/dry line as a proxy an acceptable representation of the shoreline (Hoeke et al., 2001; Moore, 2000; Overton et. al, 1999; Plant and Holman, 1997; Shoshany and Degani, 1992; Thieler and Danforth, 1994). This is especially true when the imagery is collected during the same season when the same wave and wind climate can be expected to exist at a particular study site, as well as locations, such as Bay St. Louis, where there is not a large tidal range impact (Gens, 2010; Leatherman, 2003; Table 4.6).

Bars not only attenuate the waves as they approach the beach, but they also influence the currents in the area, as well as the amount of sediment distributed along the shore (Masselink et al., 2011; Wijnberg and Kroon, 2002). This can be visualized at Bay St. Louis, where the beach width varied between accretion in the westernmost and center sections (0.5%) and erosion in the easternmost portion (-16.2%). This can be due to number of nearshore bars identified in each area. The easternmost portion had a smaller number of bars identified, which could have reduced the protection the beach and dunes received against high energy events, in turn producing more erosion in this area. Meanwhile, the westernmost and center portion of the study site, which had more identified nearshore bars, was more likely better protected from the high-energy wave events. If volumetric data were available, we would be able to trace the sand movements between the dune, beach and bars. This study

is also limited in investigating the volumetric changes caused by sediment distribution along the systems since pre- and post-events volumetric data were not available for any of the sites. Despite this limitation, the analysis demonstrated that nearshore bars are intrinsically connected to the system and that their presence and morphology influence how dunes and bars respond to high-energy wave events.

Understanding the relationship between bars, beach, and dunes and how variations of the bar shape influence beach and dune characteristics is important for improving beach ecosystem services and for coastal management. By studying and analyzing nearshore bar morphology, coastal managers can identify hotspots of erosion at their locations investing more resources to protect those areas and infrastructures when a high-energy wave events approach. Also, as discussed previously, crescentic and discontinuous longshore bars may aid in the generation of rip currents (Bruneau et al., 2009; Castelle et al., 2016; Castelle and Coco, 2012; Dalrymple et al., 2011). The findings of this paper suggest that identifying what type of bar is present, as well as the corresponding beach and dune morphology, can help aid identify dangerous spots for swimmers and beachgoers due to topographic rip currents.

This research, and future similar research, heavily relies on the availability of satellite imagery immediately following the high-energy wave events, specifically in the case of winter storms. For tropical cyclones agencies usually acquire imagery pre- and post-event, these procedures are not followed for winter storms, as well as the variability of the tidal range at the time the image was taken. This limitation could be minimized in future studies by combining satellite imagery with drone flyovers (Klemas, 2011; Seymor et al., 2018; Turner et al., 2016). Small Unmanned Aircraft Systems (sUAS) imagery could supplement the dataset and allow for improved analysis of system response to multiple events and inter-

event comparison. These types of studies would also benefit from having more localized *in situ* weather data to better identify and characterize the high-energy wave events. The use of sUAS has also allowed larger spatial and temporal coverage of volumetric data collection of coastal environments at lower costs (Colomina and Molina, 2014; Klemas, 2015; Seymour et al., 2017). Adding volumetric data to similar future studies will allow researchers to investigate how sand is redistributed across the entire coastal system (dune, beach, and bars) during high energy events.

Based on our results, we can also determine that even though the three study sites have different wave climates and geomorphic characteristics, the morphology of the bar is an important component of the coastal system that can determine how the beach-dune system responds to high-energy wave events. The site at Duck, NC had a discontinuous longshore bar that somewhat protected the coastal system, but still produced hotspots of erosion were the gaps of the bars were located. Cassino Beach, RS had a continuous longshore bar and had better protection from high-energy wave events. Bay St. Louis presented little to no changes because it has a robust multiple bar system that protected the beach. Future studies should consider storm clusters similar to Angnuureng et al. (2017) to further understand how the repeated high-energy wave events influence nearshore bar behavior and beach-dune responses.

5 Conclusions

This research discusses the importance of studying coastal systems through a holistic approach. Applying the rule-based classification method in Chapter 3, we identified changes in the beach, dunes, and nearshore bars and established concrete process-based linkages to the coastal system holistically. Understanding how the dunes, beach, and bars' dynamics are

related, and how each component affects the response of the other during storm conditions, will significantly improve the way that we manage, protect, and develop our coastlines.

We defined high-energy wave events as those producing wave heights exceeding the site's significant wave height ($H_{s\text{-}site}$) (Hill et al., 2004; Splinter et al., 2014) and lasting longer than 6 hours. Pre- and post-events images were analyzed using a rule-base classification according to Chapter 3. Results showed that the morphology of nearshore bars have a direct impact on how the beach-dune system responds to high-energy wave events such as tropical cyclones and winter storms. The results showed that the morphology of the bar can determine the response of the dune-beach complex. We suggest that future studies would benefit from the inclusion of drone use to streamline the process of assessing and monitoring coastal landscapes and focus on how storm clusters may influence nearshore bar behavior and beach-dune responses. Drones and sUASs are becoming more popular and demand have caused their price to be significantly reduced, providing a cost-effective tool for coastal scientists and mangers to continue their work at these sites.

CHAPTER 5

CONCLUSIONS

This dissertation research focused in developing a new low-cost approach for nearshore bars that integrates multispectral imagery. Nearshore bar research will benefit from the larger spatial scale provided by satellite sensors, since we will be able to study complete systems instead of partial segments. Larger spatial scale and remote sensing capabilities also will allow scientists to study systems that previously have been considered inaccessible. A systems approach was utilized to study the interactions of the nearshore dynamics and the beach-dune system. The results garnered could improve the ability of coastal managers and scientists to monitor and manage coastlines.

Chapter 2 offered a comprehensive review of the current methods available to remotely detect nearshore bars. This chapter investigated near-Earth and satellite imagery remotely based observations that have been used to study nearshore bars. It also delves into how several recent advances in technology and techniques allow the remote measurement of bar width and height, beach slope, shoreline orientation, and bar count. Finally, the chapter includes a discussion on how video monitoring systems are presently the most popular method to derive nearshore bar data, however spatial prediction models using satellite imagery can also provide reliable bar morphodynamic information.

Chapter 3 tests the first hypothesis of the dissertation, which is the generation and validation of a new approach to identify nearshore bars using multispectral imagery. A rule-based classification approach was created to ascertain bar characteristics at a

dissipative (Bay St. Louis, MS and Cassino Beach, BRA) and an intermediate (Duck, North Carolina) beach. The identification approach was validated using results obtained from Argus video monitoring systems. The information derived from utilizing a rule-based classification to extract nearshore bar characteristics from multispectral imagery can provide important data of the spatio-temporal scale at which nearshore bar systems evolve. Single and multiple bar systems were identified and characterized at three locations. The use of this approach is possible thanks to advancements in satellite sensors and imagery with the advancements in VHR multispectral imagery.

Lastly, Chapter 4 delves into the second hypothesis of the dissertation, which seeks to understand how bar morphology influences beach-dune characteristics and how this relationship varies geographically. Results showed that the morphology of the bars (longshore bars, discontinuous longshore bars, or crescentic bars) can impact on how the beach-dune system responds to high-energy wave events. These results did not vary per location meaning that the morphology of the bar is what determines response of the dune-beach complex. The site at Duck, NC had a discontinuous longshore bar that somewhat protected the coastal system, but still produced hotspots of erosion were the gaps of the bars were located. Cassino Beach, RS had a continuous longshore bar and had better protection from high-energy wave events. Bay St. Louis presented little to no changes because it has a robust multiple bar system that protected the beach.

This dissertation provides important methodological and theoretical knowledge on nearshore bar studies. Understanding how dunes, beach and bars dynamics are related and how each component affects the response of the other during high-energy wave event conditions will substantially improve the way we manage, protect, and develop our

coastlines. Future research could aim to ascertain the research value of using multispectral imagery and UAV derived imagery, a cost effective and less invasive method of coastal monitoring, to study and characterize nearshore bar morphodynamics. This future study would look into integrating traditional remote sensing technology (multispectral imagery) with contemporary innovative techniques (i.e. UAV, drones) for coastal management and studies. Future studies should also consider investigating how repeated high-energy wave events, or high-energy wave event clusters, influence nearshore bar behavior and beach-dune responses.

REFERENCES

Aagaard, T., Davidson-Arnott, R., Greenwood, B., Nielsen, J., 2004. Sediment supply from shoreface to dunes: Linking sediment transport measurements and long-term morphological evolution. Geomorphology 60, 205–224.

Aagaard, T., Kroon, A., Andersen, S., Möller Sørensen, R., Quartel, S., and Vinther, N., 2005. Intertidal beach change during storm conditions; Egmong, The Netherlands. Marine Geology. 218, 65-80.

Aagaard, T., Hughes, M., 2010. Breaker turbulence and sediment suspension in the surf zone. Mar. Geol. 271, 250-259.

Aarninkhof, S.G.J., Caljouw, M., Stive, M.J.F., 2000. Video-based, quantitative assessment of intertidal beach variability. Coast. Eng. 3291–3304.

Aarninkhof, S.G.J., Turner, I.L., Dronkers, T.D.T., Caljouw, M., Nipius, L., 2003. A video-based technique for mapping intertidal beach bathymetry. Coast. Eng. 49, 275–289.

Angnuureng, D. B., Almar, R., Senechal, N., Castelle, B., Addo, K. A., Marieu, V., & Ranasinghe, R. 2017. Shoreline resilience to individual storms and storm clusters on a meso-macrotidal barred beach. *Geomorphology*, *290*, 265-276.

Aleman, N., Certain, R., Robin, N., Barusseau, J.P., 2017. Morphodynamics of slightly oblique nearshore bars and their relationship with the cycle of net offshore migration. Mar. Geol. 392, 41-52.

Aleman, N., Robin, N., Certain, R., Vanroye, C., Barusseau, J.-P., Bouchette, F., 2011. Typology of nearshore bars in the Gulf of Lions (France) using LIDAR technology. J. Coast. Res. 721–725.

Alexander, P.S., Holman, R.A., 2004. Quantification of nearshore morphology based on video imaging. Mar. Geol. 208, 101–111.

Almar, R., Castelle, B., Ruessink, B.G., Sénéchal, N., Bonneton, P., Marieu, V., 2009. High-frequency video observation of two nearby double-barred beaches under high-energy wave forcing. J. Coast. Res. SI56, 1706-1710.

Archetti, R., Zanuttigh, B., 2010. Integrated monitoring of the hydro-morphodynamics of a beach protected by low crested detached breakwaters. Coast. Eng. 57, 879–891.

Armaroli, C., Ciavola, P., 2011. Dynamics of a nearshore bar system in the northern Adriatic: A video-based morphological classification. Geomorphology 126, 201–216.

Armaroli, C., Ciavola, P., Caleffi, S., Gardelli, M., 2006. Morphodynamics of Nearshore Rythmic forms: an energy-based classification, in: Proceeding International Conference of Coastal Engineers 2006 San Diego , USA. San Diego, pp. 1–14.

Bapentire, D., Almar, R., Senechal, N., Castelle, B., Appeaning, Addo, K., Marieu, V., Ranasinghe, R., 2017. Shoreline resilience to individual storms and storm clusters on a meso-macrotidal barred beach. Geomorphology 290, 265-276.

Bauer, B.O., 1991. Aeolian decoupling of beach sediments. Annals Assoc. Americ. Geog. 81, 290-303.

Bauer, B., Greenwood, B., 1990. Modification of a linear bar-trough system by a standing edge wave. Mar. Geol., 177-294.

Barbier, E.B., Koch, E.W., Silliman, B.R., Hacker, S.D., Wolanski, E., Primavera, J., Granek, E.F., Polasky, S., Aswani, S., Cramer, L.A., Stoms, D.M., Kennedy, C.J., Bael, D., Kappel, C.V. Perillo, G.M.E., Reed, D.J., 2008. Coastal ecosystem-based management with nonlinear ecological functions and values. Science 319, 321-323.

Bergsma, E.W.J., Conley, D.C., Davidson, M.A., O'Hare, T.J., 2016. Video-based nearshore bathymetry estimation in macro-tidal environments. Mar. Geol. 374, 31–41.

Beyer, H.A., 1992. Accurate calibration of CCD-cameras. Proc. 1992 IEEE Comput. Soc. Conf. Comput. Vis. Pattern Recognit. 96–101.

Bird, E.C.F. 1993. Submerging coasts. Chichester: John Wiley.

Birkemeier, W.A., 1985. Time scales of nearshore profile change, in: 19th International Conference on Coastal Engineering. ASCE, New York, pp. 1507–1521.

Birkemeier, W.A., Mason, C., 1984. The CRAB: A unique nearshore surveying vehicle. J. Surv. Eng. 110, 1-7.

Blaschke, T. 2010. Object based image analysis for remote sensing. ISPRS Journal of Photogrammetry and Remote Sensing. 65, 2-16.

Blaschke, T., Hay, G.J. 2001. Object-oriented image analysis and scale-space: theory and mehods for modeling and evaluating multiscale landscape structure. International

Archives of Photogrammetry and Remote Sensing. 34, 22-29.Boak, E., Turner, I.L., 2005. Shoreline definition and detection: a review. J. Coast. Res. 21, 688-703.

Blaschke, T., Hay, G.J., Kelly, M., Lang, S., Hofmann, P., Addink, E., Feitosa, R.Q., Van der Meer, F., Van der Werff, H., Van Coillie, F., 2014. Geographic object-based image analysis–towards a new paradigm. ISPRS J. Photogramm. Remote Sens. 87, 180–191.

Borja, A., 2005. The European water framework directive: A challenge for nearshore, coastal and continental shelf research. Cont. Shelf Res. 25, 1768-1783.

Bouziani, M., Goita, K., & He, D. C. 2010. Rule-based classification of a very high resolution image in an urban environment using multispectral segmentation guided by cartographic data. *IEEE Transactions on Geoscience and Remote Sensing*, *48*(8), 3198-3211.

Bracs, M.A., Turner, I.L., Splinter, K.D., Short, A.D., Lane, C., Davidson, M.A., Goodwin, I.D., Pritchard, T., Cameron, D., 2016. Evaluation of Opportunistic Shoreline Monitoring Capability Utilizing Existing "Surfcam" Infrastructure. J. Coast. Res. 32, 542–554.

Brignone, M., Schiaffino, C.F., Isla, F.I., Ferrari, M., 2012. A system for beach video-monitoring: Beachkeeper plus. Comput. Geosci. 49, 53–61.

Carter, R.W.G., Balsillie, J.H., 1983. A note on the amount of wave energy transmitted over nearshore sand bars. Earth Surf. Process. Landforms 8, 213–222.

Carter, R.W.G., Kitcher, K.. J., 1979. The Geomorphology of Offshore Sand Bars on the North Coast of Ireland, in: Proceedings of the the Royal Irish Academy: Section B, Geological and Chemical Science. pp. 43–61.

Castelle, B., Marieu, V., Bujan, S., Splinter, K. D., Robinet, A., Sénéchal, N., & Ferreira, S. 2015. Impact of the winter 2013–2014 series of severe Western Europe storms on a double-barred sandy coast: Beach and dune erosion and megacusp embayments. *Geomorphology*, *238*, 135-148.

Cheng, G., Han, J., Guo, L., Liu, Z., Bu, S., Ren, J., 2015. Effective and efficient midlevel visual elements-oriented land-use classification using VHR remote sensing images. IEEE Trans. Geosci. Remote Sens. 53, 4238–4249.

Clark, J.R. 1997. Coastal zone management for the new century. Ocean and Coastal Management. 37,2, 191-216.

Coastal Zone Management Act, 16 U.S.C. § 1451, section 302

Coco, G., Payne, G., Bryan, K.R., Rickard, D., Ramsay, D., Dolphin, T., 2005. The use of imaging systems to monitor shoreline dynamics, in: Proceedings of the 1st International Conference on Coastal Zone Management and Engineering in the Middle East. pp. 1–7.

Cohn, N., Ruggiero, P., Ortiz, J., Walstra, D.J., 2014. Investigating the Role of Complex Sandbar Morphology on Nearshore Hydrodynamics. J. Coast. Res. 54–59.

Davidson-Arnott, R. 2010. Introduction to coastal processes and geomorphology. Cambridge University Press.

Davidson-Arnott, R.G.D., 2013. Nearshore bars. In: Shroder, J. (Editor in Chief), Sherman, D.J. (Ed), Treatise on Geomorphology. Academic Press, San Diego, CA, vol.10, Coastal Geomorphology, 10-148.

Davidson-Arnott, R. G., & Law, M. N. 1996. Measurement and prediction of long-term sediment supply to coastal foredunes. *Journal of Coastal Research*, 654-663.

Davidson, M., Van Koningsveld, M., de Kruif, A., Rawson, J., Holman, R., Lamberti, A., Medina, R., Kroon, A., Aarninkhof, S., 2007. The CoastView project: Developing video-derived Coastal State Indicators in support of coastal zone management. Coast. Eng. 54, 463–475.

Dean, R.G., 1991. Equilibrium beach profiles: characteristics and applications. J. Coast. Res. 7, 53-84.

Dehouck, A., Martiny, N., Froudefond, J.M., Sénéchal, N., Bujan, S., 2009. New outcomes from spatial remote sensing during the ECROS experiment : towards validation of ocean color products and large-scale bathymetry mapping in a coastal zone. J. Coast. Res. 1756–1760.

Dolan, T.J., Dean, R.G., 1985. Multiple Longshore Sand Bars in the Upper Chesapeake Bay. Estuar. Coast. Shelf Sci. 21, 727–743.

Dorsch, W., Newland, T., Tassone, D., Tymons, S., & Walker, D. 2008. A statistical approach to modelling the temporal patterns of ocean storms. *Journal of Coastal Research*, 1430-1438.

Dugan, J.E., Airoldi, L., Chapman, M.G., Walker, S.J., Schlacher, T., 2011. 8.02 Estuarine and coastal structures: environmental effects, a focus on shore and nearshore structures. Treatise on Estuarine and Coastal Science, 8, 17-41.

Ehrlich, D., Guo, H.D., Molch, K., Ma, J.W., Pesaresi, M., 2009. Identifying damage caused by the 2008 Wenchuan earthquake from VHR remote sensing data. Int. J. Digit. Earth 2, 309–326.

Elgar, S., Gallagher, E.L., Guza, R.T., 2001. Nearshore sandbar migration. J. Geophys. Res. 106, 11623-11627.

Elko, N., Holman, R., 2014. The past and future of nearshore processes research: Reflections on the Sallenger years and a new vision for the future. Shore and Beach 82, 30–31.

Evans, O.F., 1940. The low and ball of the eastern shore of Lake Michigan. J. Geol. 48, 476-511.

Falqués, A., Dodd, N., Garnier, R., Ribas, F., MacHardy, L.C., Larroudé, P., Calvete, D., Sancho, F., 2008. Rythmic surf zone bars and morphodynamic self-organization. Coastal Engineering. 55, 622-641.

French, J.R., Burningham, H., 2009. Coastal geomorphology: trends and challenges. Prog. Phys. Geogr. 33, 117–129.

French, J. R., & Burningham, H. 2011. Coastal geomorphology. *Progress in Physical Geography*, *35*(4), 535-545.

French, J.R. and H. Burningham, 2013. Coasts and climate, Insights from geomorphology. Progress in Physical Geography 37, 4, 550-561.French, J.R., Burningham, H., 2011. Coastal geomorphology. Prog. Phys. Geogr. 35, 535–545.

Gallagher, E.L., Elgar, S., Guza, R.T., 1998. Observations of sand bar evolution on a natural beach. J. Geophys. Res. 103, 3203–3215.

Gama, C., Fortes, C.J.E.M., Baptista, P., Albardeiro, L., Pinheiro, L., Salgado, R., 2011. Medium-term evolution of an intermediate beach with an intertidal bar (Amoreira beach, Southwest Portuguese rocky coast). J. Coast. Res. SI 64, 80-84.

Garnier, R., Medina, R., Pellón, E., Falqués, A., Turki, I., 2012. Intertidal finger bars at El Puntal Spit, Bay of Santander, Spain. Coastal Engineering, 1-8.

Gens, R. 2010. Remote sensing of coastlines: detection, extraction and monitoring. *International Journal of Remote Sensing*, *31*(7), 1819-1836.

Greenwood, B., Davidson-Arnott, R.G.D., 1979. Sedimentation and equilibrium in wave-formed bars: a review and case study. Can. J. Earth Sci. 16, 312–332.

Greenwood, B., Richards, R.G., Brander, R.W., 1995. Acoustic imaging of sea-bed geometry: A High resolution remote tracking sonar (HRRTS II). Mar. Geol. 112, 207-218.

Guedes, R.M.C., Calliari, L.J., Holland, K.T., Plant, N.G., Pereira, P.S., Alves, F.N.A., 2011. Short-term sandbar variability based on video imagery: Comparison between Time-Average and Time-Variance techniques. Mar. Geol. 289, 122–134.

Harris, W.D., Umbach, M.J., 1972. Underwater mapping. Photogramm. Eng. 34, 765–772.

Hesp, P., 1988. Surfzone, beach, and foredune interactions on the Australian Southeast coast. J. Coast. Res. 15–25.

Hesp, P. A. 2012. Surfzone-beach-dune interactions. 35-40.

Heumann, B.W. 2011. An Object-Based Classification of Mangroves Using a Hybrid Decision Tree - Support Vector Machine Approach. Remote Sensing. 3, 2440-2460.

Heuvelink, G.B.M., 2005. Propagation of Error in Spatial Modeling with GIS, in: Ley, Goodenild, Maguire, Rhind (Eds.), Geographical Information Systems Volume 1 Principles and Technical Issues. pp. 207–217.

Holland, K.T., Holman, R.A., Lippmann, T.C., Stanley, J., Plant, N.G., 1997. Practical Use of Video Imagery in Nearshore Oceanographic Field Studies. J. Geophys. Res. 22, 81–92.

Holman, R.A., Haller, M.C., 2013. Remote Sensing of the Nearshore. Ann. Rev. Mar. Sci. 5, 95–113.

Holman, R.A., Stanley, J., 2007. The history and technical capabilities of Argus. Coast. Eng. 54, 477–491.

Holman, R. A, Haller, M.C., Lippmann, T.C., Holland, K.T., Jaffe, B.E., 2015. Advances in nearshore processes research: Four decades of progress. Shore and Beach 83, 39–52.

Holman, R., Stanley, J., Özkan-haller, T., 2003. Applying Video Sensor Network to Nearshore Environment Monitoring. IEEE Pervasive Comput. 14–21.

Houser, C., Hapke, C., & Hamilton, S. 2008. Controls on coastal dune morphology, shoreline erosion and barrier island response to extreme storms. *Geomorphology*, *100*(3-4), 223-240.

Houser, C., 2009. Synchronization of transport and supply in beach-dune interaction. Progress Phys. Geog. 33, 733-746.

Houser, C., Hamilton, S., 2009. Sensitivity of post-hurricane beach and dune recovery to event frequency. Earth Surface Processes and Landforms 34, 613-628.

Houser, C., Ellis, J., 2013. Beach and dune interaction. In: Shorder, J. (Editor in Chief), Sherman, D.J. (Ed.), Treatise on Geomorphology. Academic Press, San Diego, CA, vol. 10, Coastal Geomorphology, 267-288.

Houser, C., Greenwood, B., 2007. Onshore Migration of a Swash Bar During a Storm. J. Coast. Res. 231, 1–14.

Jahjah, M., Ulivieri, C., 2010. Automatic archaeological feature extraction from satellite VHR images. Acta Astronaut. 66, 1302–1310

Jensen, J.R., 2005. Introductory Digital Image Processing: A Remote Sensing Perspective. 3rd Ed. Pearson, Upper Saddle River, NJ.

Jensen, S.G., Aagaard, T., Baldock, T.E., Kroon, A., Hughes, M., 2009. Berm formation and dynamics on a gently sloping beach; the effect of water level and swash overtopping. Earth Surf. Process. Landforms 34, 1533–1546.

King, C.A.M., Williams, W.W., 1949. The formation and movement of sand bars by wave action. The Geographical Journal 113, 70-85.

Kingston, K.S., Ruessink, B.G., Van Enckevort, I.M.J., Davidson, M.A., 2000. Artificial neural network correction of remotely sensed sandbar location. Mar. Geol. 169, 137–160.

Klemas, V., 2011. Remote Sensing Techniques for Studying Coastal Ecosystems: An Overview. J. Coast. Res. 27, 2–17.

Komar, P.D., 1998. Beach processes and sedimentation. Prentice Hall, Upper Saddle River, NJ.

Konicki, K.M., Holman, R.A., 2000. The statistics and kinematics of transverse sand bars on an open coast, Marine Geology.

Lafon, V., De Melo Apoluceno, D., Dupuis, H., Michel, D., Howa, H., Froidefond, J.M., 2004. Morphodynamics of nearshore rhythmic sandbars in a mixed-energy environment (SW France): I. Mapping beach changes using visible satellite imagery. Estuar. Coast. Shelf Sci. 61, 289–299.

Lafon, V., Froidefond, J.M., Lahet, F., Castaing, P., 2002. SPOT shallow water bathymetry of a moderately turbid tidal inlet based on field measurements. Remote Sens. Environ. 81, 136–148.

Larson, M., Kraus, N.C., 1994. Temporal and spatial scales of beach profile change, Duck, North Carolina. Mar. Geol. 117, 75-94.

Leatherman, S. P. 2003. Shoreline change mapping and management along the US East Coast. *Journal of Coastal Research*, 5-13.

Lee, Z., Carder, K.L., Mobley, C.D., Steward, R.G., Patch, J.S., 1999. Hyperspectral remote sensing for shallow waters: 2. Deriving bottom depths and water properties by optimization. Appl. Opt. 38, 3831–43.

Lippmann, T.C., Holman, R.A., 1989. Quantification of sand bar morphology: A video technique based on wave dissipation. J. Geophys. Res. Ocean. 94, 995–1011.

Lippmann, T.C., Holman, R. A., 1990. The spatial and temporal variability of sand bar morphology. J. Geophys. Res. 95, 11575-11590.

List, J.H., Farris, A.S., 1999. Large-scale shoreline response to storms and fair weather. Proceedings Coastal Sediments '99, American Society of Civil Engineering, Reston, VA, 1324-1338.

List, J.H., Farris, A.S., and Sullivan, C., 2006. Reversing storm hotspots on sandy beaches, Spatial and temporal characteristics. Marine Geology, 226, 261-279.

Liu, H., Sherman, D., Gu, S., 2007. Automated extraction of shorelines from airborne light detection and tanging data and accuracy assessment based on Monte Carlo simulation. Journal of Coastal Research. 6, 1359-1369.

López, I., Aragonés, L., Villacampa, Y., Serra, J.C., 2017. Neural network for determining the characteristic point of the bars. Ocean Engineering. 136, 141-151.

Lundahl, A.C., 1948. Underwater depth determination by aerial photography. Photogramm. Eng. 14, 454–462.

Madsen, A.J., Plant, N.G., 2001. Intertidal beach slope predictions compared to field data. Mar. Geol. 173, 121–139.

Masselink, G., Aagaard, T., Kroon, A, 2011. Destruction of intertidal bar morphology during a summer storm surge event: Example of positive morphodynamic feedback. J. Coast. Res. 105–109.

Masselink, G., Austin, M., Scott, T., Poate, T., Russell, P., 2014. Role of wave forcing, storms and NAO in outer bar dynamics on a high-energy, macro-tidal beach. Geomorphology 226, 76–93.

Masselink, G., Kroon, A., Davidson-Arnott, R.G.D., 2006. Morphodynamics of intertidal bars in wave-dominated coastal settings - A review. Geomorphology 73, 33–49.

Masselink, G., & Short, A. D. (1993). The effect of tide range on beach morphodynamics and morphology: a conceptual beach model. *Journal of coastal research*, 785-800.

McNinch, J.E., 2007. Bar and swash imaging radar (BASIR): A mobile X-band radar designed for mapping nearshore sand bars and swash-defined shorelines over large distances. J. Coast. Res. 59–74.

Mei, C.C., 1985. Resonant reflection of surface waves by periodic sand bars, J. Fluid Mech. 152, 315-335.

Mole, M.A., Mortlock, T.R., Turner, I.L., Goodwin, I.D., Splinter, K.D., Short, A.D., 2013. Capitalizing on the surfcam phenomenon: a pilot study in regional-scale shoreline monitoring utilizing existing camera infrastructure. J. Coast. Res. SI65, 1433–1438.

Monteys, X., Harris, P., Caloca, S., Cahalane, C., 2015. Spatial prediction of coastal bathymetry based on multispectral satellite imagery and multibeam data. Remote Sens. 7, 13782–13806.

Moore, L.J., 2000. Shoreline Mapping Techniques. J. Coast. Res. 16, 111–124.

Moore, L.J., Sullivan, C., Aubrey, D.G., 2003. Interannual evolution of multiple longshore sand bars in a mesotidal environment, Truro, Massachusetts, USA. Mar. Geol. 196, 127–143.

Morton, R., Paine, J.G., and Gibeaut, J.C., 1994. Stages and durations of post-storm beach recovery, southeastern Texas coast, U.S.A. Journal of Coastal Research 10,4, 884-908.

Morton, R.A., Sallenger, A.H. 2003. Morphological impacts of extreme storms on sandy beaches and barriers. Journal of Coastal Research. 19, 560-573.

Murray, T., Cartwright, N., Tomlinson, R., 2013, Video-imaging of transient rip currents on the Gold Coast open beaches. J. Coast. Res. SI65, 1809-1814.

Nieto, M.A., Garau, B., Balle, S., Simarro, G., Zarruk, G.A., Ortiz, A., Tintoré, J., Álvarez-Ellacuría, Gómez-Pujol, L., Orfila, A., 2010. An open source, low cost video-based coastal monitoring system. Earth Surf. Process. Landforms 35, 1712–1719.

Nordstrom, K.F., Gares, P.A., 1990. Changes in the volume of coastal dunes in New Jersey, USA. Ocean and Shoreline Management 14, 1-10.

Orme, A.R., 2013. The four traditions of coastal geomorphology. In, Shroder, J. (Editor in Chief), Sherman, D.J. (Ed.), Treatise on Geomorphology. Academic Press, San Diego, CA, vol. 10, Coastal Geomorphology, pp. 5-38.

Penna, M.A., 1991. Camera calibration: A quick and easy way to determine the scale factor. IEEE Trans. Pattern Anal. Mach. Intell. 13, 1240–1245.

Phillips, M.S., Harley, M.D., Turner, I.L. Splinter, K.D., Cox, R.J. 2017. Shoreline recovery on wave-dominated sandy coastlines: the role of sandbar morphodynamics and nearshore wave parameters. Marine Geology. 385, 146-159.

Plant, N.G., Aarninkhof, S.G.J., Turner, I.L., Kingston, K.S., 2007. The Performance of Shoreline Detection Models Applied to Video Imagery. J. Coast. Res. 233, 658–670.

Plant, N.G., Holland, K.T., Puleo, J.A., 2002. Analysis of the scale of errors in nearshore bathymetric data. Mar. Geol. 191, 71–86.

Plant, N.G., Holman, R.A., 1997. Intertidal beach profile estimation using video images. Mar. Geol. 140, 1–24.

Price, T.D., Rutten, J., Ruessink, B.G. 2011. Coupled behavior within a double sandbar system. Journal of Coastal Research. SI 64, 125-129.

Pye, K., 1982. Morphological development of coast dunes in a humid tropical environment, Cape Bedford and Cape Flattery, North Queensland. Phys. Geog. 64, 213-227.

Ranasinghe, R., Symonds, G., Black, K., and Holman, R., 2004. Morphodynamics of intermediate beaches, a video imaging and numerical modelling study. Coastal Engineering, 51.

Rangel-Buitrago, N., & Anfuso, G. 2011. An application of Dolan and Davis (1992) classification to coastal storms in SW Spanish littoral. *Journal of Coastal Research*, 1891-1895.

Reyf, V., Davies, A.G., Belzons, M., 1995. On the formation of bars by the action of waves on an erodible bed: A laboratory study. J. Coast. Res. 11, 1180-1194.

Ribas, F., Falqués, A., Garnier, R., 2017. Nearshore sand bars on western Mediterranean beaches. In *Atlas of Bedforms in the Western Mediterranean* (pp. 81-88). Springer, Cham.

Ribas, F., Ojeda, E., Price, T.D., Guillén, J., 2010. Assessing the suitability of video imaging for studying the dynamics of nearshore sandbars in tideless beaches. IEEE Trans. Geosci. Remote Sens. 48, 2482–2497.

Rihouey, D., Dugor, J., Dailloux, D., Morichon, D., 2009. Application of remote sensing video system to coastal defense monitoring. J. Coast. Res. SI56, 1582-1586.

Rodríguez-Martín, R., Rodríguez-Santalla, I., 2013. Detection of Submerged Sand Bars in the Ebro Delta Using Aster Images, in: New Frontiers in Engineering, Geology and the Environment. pp. 103–106.

Roelvink, J.A., Stive, M.J.F., 1989. Bar-generating cross-shore flow mechanisms on a beach. J. Geophys. Res. 94, 4785-4800.

Román-Rivera, M.A., 2014. Spatial and Temporal Evaluation of Dune, Beach and Nearshore Bar Interactions Cape. Thesis. East Carolina University, Greenville, North Carolina, USA.

Román-Rivera, M.A., Ellis, J.T., 2019. A synthetic review of remote sensing applications to detect nearshore bars. Mar. Geol. 408, 144–153. doi:10.1016/j.margeo.2018.12.003

Ruessink, B.G., Bell, P.S., van Enckevort, I.M.J., Aarninkhof, S.G.J., 2002. Nearshore bar crest location quantified from time-averaged X-band radar images. Coast. Eng. 45, 19-32.

Ruessink, B. G., & Jeuken, M. C. J. L. 2002. Dunefoot dynamics along the Dutch coast. *Earth Surface Processes and Landforms: The Journal of the British Geomorphological Research Group*, *27*(10), 1043-1056.

Ruessink, B.G., Kroon, A. 1994. The behavior of a multiple bar system in the nearshore of Tereschelling, the Netherlands: 1965-1993. Marine Geology. 121 (3), 187-197.

Rutten, J., Ruessink, B.G., Price, T.D., 2018. Observations on sandbar behavior along a man-made curved coast. ESPL. 43, 134-149.

Sallenger, A.H., Howard, P.C., Fletcher III, C.H., Howd, P.A., 1983. A system for measuring bottom profile, waves and currents in the high-energy nearshore environment. Mar. Geol. 51, 63-76.

Schiaffino, C.F., Brignone, M., Corradi, N., Cevasco, A., Iannotta, M.A., Cavallo, C., Ferraro, M., 2013. The Ligurian webcam network and database for coastal management. Coastal Erosion Monitoring, 79.

Senechal, N., Coco, G., Castelle, B., Marieu, V., 2015. Storm impact on the seasonal shoreline dynamics of a meso- to macrotidal open sandy beach (Biscarrosse, France). Geomorphology 228, 448–461.

Sallenger Jr., A.H., Krabill, W.B., Swift, R.N., Brock, J., List, J., Hansen, M., Holman, R.A., Manizade, S., Sontag, J., Meredith, A., Morgan, K., Yunkel, J.K. Frederick, E.B., Stockton, H., 2003. Evaluation of airborne topographic lidar for quantifying beach changes. Journal of Coastal Research, 19, 125-133.

Seymor, A.C., Ridge, J.T., Rodriguez, A.B., Newton, E., Dale, J., Johnston, D.W. 2018.

Deploying Fixed Wing Unoccupied Aerial Systems (UAS) for Coastal Morphology Assessment and Management. Journal of Coastal Research. 34(3), 704-717.

Shepard, F.P. 1950. Longshore-bars and longshore-troughs. N0. TM-15. Corps of Engineers Washington DC Beach Erosion Board.

Sheppard, C.R.C., Matheson, K., Bythell, J.C., Murphy, P., Blair Myers, C., Blake, B., 1995. Habitat mapping in the Caribbean for management and conservation: use and assessment of aerial photography. Aquat. Conserv. Mar. Freshw. Ecosyst. 5, 277–298.

Sherman, D.J., Bauer, B.O., 1993. Dynamics of beach-dune systems. Progress in Physical Geography 17, 413-447.

Short, A.D., 1975, Multiple offshore bars and standing waves. J. Geophys. Res. 80, 3838-3840.

Short, A.D., Aagaard, T., 1993. Single and multi-bar beach change models. J. Coast. Res. SI 15, 141-157.

Short, A.D., Hesp, P.A., 1982. Wave, beach and dune interactions in southeastern Australia. Mar. Geol. 48, 259–284.

Shoshany, M., Degani, A., 1992. Shoreline Detection by Digital Image Processing of Aerial Photography. J. Coast. Res. 8, 29–34.

Siegel, D. A, Wang, M., Maritorena, S., Robinson, W., 2000. Atmospheric correction of satellite ocean color imagery: the black pixel assumption. Appl. Opt. 39, 3582–91.

Simarro, G., Ribas, F., Alvarez, A., Guillen, J., Chic, O., Orfila, A., 2017. ULISES: An open source code for extrinsic calibrations and planview generations in coastal video monitoring systems. J. Coast. Res. 33, 1217-1227.

Smith, E.R., Kraus, N., 1991. Laboratory study of wave-breaking over bars and artificial reefs. J. Waterway, Port, Coastal and Ocean Engineering 117, 307-325.

Splinter, K.D., Harley, M., Turner, I., 2018. Remote Sensing is Changing Our View of the Coast: Insights from 40 Years of Monitoring at Narrabeen-Collaroy, Australia. Rem.Sen. 10, 1-25.

Splinter, K.D., Holman, R.A., Plant, N.G., 2011. A behavior-oriented dynamic model for sandbar migration and 2DH evolution. J. Geophys. Res. Ocean. 116, 1–21.

Splinter, k., Strauss, D., Tomlinson, R., 2011. Can we reliably estimate dune erosion without knowing pre-storm bathymetry?. 20th Australasian Coastal and Ocean Engineering Conference.

Splinter, K. D., Carley, J. T., Golshani, A., & Tomlinson, R. 2014. A relationship to describe the cumulative impact of storm clusters on beach erosion. *Coastal engineering*, *83*, 49-55.

Sonu, C., 1972. Field observation of nearshore circulation and meandering currents. J. Geophys. Res. 77, 3232-3247.

Stephenson, W. J., & Brander, R. W. 2003. Coastal geomorphology into the twenty-first century. *Progress in Physical Geography*, *27*(4), 607-623.

Stockdon, H.F., Sallenger Jr., A.H., List, J.H., Holman, R.A., 2002. Estimation of shoreline position and change using airborne topographic lidar data. Journal of Coastal Research, 18, 502-513.

Tarabalka, Y., Tilton, J.C., 2012. Improved hierarchical optimization-based classification of hyperspectral images using shape analysis, in: 2012 IEEE International Geoscience and Remote Sensing Symposium. IEEE, pp. 1409–1412.

Tatui, F., Vespremeanu-Stroe, A., Ruessink, G.B., 2016. Alongshore variability of cross-shore bar behavior on a nontidal beach. Earth Surf. Process. Landforms 41, 2085–2097.

Teodoro, A.C., 2016. Optical Satellite Remote Sensing of the Coastal Zone Environment -- An Overview, in: Marghany, M. (Ed.), Environmental Applications of Remote Sensing. InTech, pp. 165–196. doi:10.5772/60828

Thia-Eng, C. 1993. Essential elements of integrated coastal zone management. Ocean and Coastal Management, 21, 81-108.

Thieler, E.R., Danforth, W.W., 1994. Historical Shoreline Mapping (I): Improving Techniques and Reducing Positioning Errors. J. Coast. Res. 10, 549–563.

Thornton, E., Humiston, R., Birkemeier, W., 1996. Bar-trough generation on a natural beach. J. Geophys. Res. 101, 12097-12110.

Turner, I.L., Aarninkhof, S.G.J., Holman, R.A., 2006. Coastal imaging applications and research in Australia. J. Coast. Res. 22, 542–555.

Turner, I. L., Harley, M. D., & Drummond, C. D. 2016. UAVs for coastal surveying. *Coastal Engineering*, *114*, 19-24.

van Dongeren, A., Plant, N., Cohen, A., Roelvink, D., Haller, M.C., Catalán, P., 2008. Beach Wizard: Nearshore bathymetry estimation through assimilation of model computations and remote observations. Coast. Eng. 55, 1016–1027.

van de Lageweg, W.I., Bryan, K.R., Coco, G. Ruessink, B.G., 2013. Observations of shoreline-sandbar coupling on an embayed beach. Mar. Geol. 344, 101-114.

van Enckevort, I.M.J., Ruessink, B.G., 2003. Video observations of nearshore bar behaviour. Part 1: Alongshore uniform variability. Cont. Shelf Res. 23, 501–512.

van Enckevort, I.M.J., Ruessink, B.G., Coco, G., Suzuki, K., Turner, I.L., Plant, N.G., Holman, R.A., 2004. Observations of nearshore crescentic sandbars. J. Geophys. Res. C Ocean. 109, 1–17.

Van de Lageweg, W. I., Bryan, K. R., Coco, G., & Ruessink, B. G. 2013. Observations of shoreline–sandbar coupling on an embayed beach. *Marine Geology*, *344*, 101-114.

Wang, Q., Liu, S., Chanussot, J., Li, X., 2018. Scene classification with recurrent attention of VHR remote sensing images. IEEE Trans. Geosci. Remote Sens. 1–13.

Wiegel, R.L., 1947. Recognition of underwater obstructions from aerial photographs. University of California, Department of Engineering.

Wijnberg, K.M., Holman, R.A., 1997. Cyclic Bar Behavior Viewed by Video Imagery, in: Coastal Dynamics ’97. pp. 375–384.

Wijnberg, K.M., Kroon, A., 2002. Barred beaches. Geomorphology 48, 103–120.

Wijnberg, K.M., Terwindt, J.H.J., 1995. Extracting decadal morphological behavior from high-resolution , long-term bathymetric surveys along the Holland coast using eigenfunction analysis. Mar. Geol. 126, 301–330.

Wright, L.D., Short, A.D., 1984. Morphodynamic variability of surf zones and beaches: A synthesis. Mar. Geol. 56, 93–118.

Ziegler, J.M., Hayes., C.R., Tuttle, S.D., 1959. Beach changes during stoms on outer Cape Cod, Massachussetts. Journal of Geology, 17, 318-336.

APPENDIX A

MARINE GEOLOGY MANUSCRIPT COPYRIGHT RELEASE

Figure A.1 Screenshot of copyright clearance from Science Direct managers of the journal Marine Geology.